NOAA Technical Memorandum NMFS-AFSC-382

# Abundance and Distribution of Age-0 Walleye Pollock in the Eastern Bering Sea Shelf During the Bering Arctic Subarctic Integrated Survey (BASIS) in 2014

D. McKelvey and K. Williams

**U.S. DEPARTMENT OF COMMERCE**
National Oceanic and Atmospheric Administration
National Marine Fisheries Service
Alaska Fisheries Science Center

August 2018

NOAA Technical Memorandum NMFS

The National Marine Fisheries Service's Alaska Fisheries Science Center uses the NOAA Technical Memorandum series to issue informal scientific and technical publications when complete formal review and editorial processing are not appropriate or feasible. Documents within this series reflect sound professional work and may be referenced in the formal scientific and technical literature.

The NMFS-AFSC Technical Memorandum series of the Alaska Fisheries Science Center continues the NMFS-F/NWC series established in 1970 by the Northwest Fisheries Center. The NMFS-NWFSC series is currently used by the Northwest Fisheries Science Center.

This document should be cited as follows:

McKelvey, D., and K. Williams. 2018. Abundance and distribution of age-0 walleye pollock in the eastern Bering Sea shelf during the Bering Arctic Subarctic Integrated Survey (BASIS) in 2014. U.S. Dep. Commer., NOAA Tech. Memo. NMFS-AFSC-382, 48 p.

Document available: http://www.afsc.noaa.gov/Publications/AFSC-TM/NOAA-TM-AFSC-382.pdf

NOAA Technical Memorandum NMFS-AFSC-382

# Abundance and Distribution of Age-0 Walleye Pollock in the Eastern Bering Sea Shelf During the Bering Arctic Subarctic Integrated Survey (BASIS) in 2014

D. McKelvey and K. Williams

Resource Assessment and Conservation Engineering Division
Alaska Fisheries Science Center
National Marine Fisheries Service
National Oceanic and Atmospheric Administration
7600 Sand Point Way N.E.
Seattle, WA 98115

*www.afsc.noaa.gov*

**U.S. DEPARTMENT OF COMMERCE**
Wilbur L. Ross Jr., Secretary
**National Oceanic and Atmospheric Administration**
RDML Timothy Gallaudet (ret.), Acting Under Secretary and Administrator
**National Marine Fisheries Service**
Chris Oliver, Assistant Administrator for Fisheries

August 2018

**This document is available to the public through:**

National Technical Information Service
U.S. Department of Commerce
5285 Port Royal Road
Springfield, VA 22161

*www.ntis.gov*

# ABSTRACT

We conducted an acoustic-trawl (AT) survey of the eastern Bering Sea during the 2014 Bering Arctic Subarctic Integrated Survey (BASIS). Because of the mixed species assemblages in the study area, we implemented proportional allocation of backscatter to the multiple species found in the trawl catch samples, modeled after the methods used for the 2011-2012 BASIS survey analysis. The abundance of age-0 walleye pollock (*Gadus chalcogrammus*) was estimated by combining acoustic measurements, the acoustic scattering properties of the dominant organisms, and the relative proportions of animals from trawl samples. Our survey results found that age-0 pollock dominated the near-surface and midwater fishes by number and we estimate their numerical abundance at $6.85 \times 10^{11}$ fish. This estimate is approximately 9 times higher than what was reported in 2011 and 3.5 times higher than what was reported in 2012. Nearly half of the overall age-0 abundance was observed in the upper 30 m of the water column. Spatially, the highest numerical densities of age-0 pollock were observed where bottom depths were less than 75 m. Sensitivity analyses indicated that both the method used to assign length and species composition from trawl hauls to backscatter (expert assignment versus using the nearest haul) had a relatively modest impact on our estimates of age-0 pollock abundance. However, both the use of 1) a trawl selectivity function to account for escapement of small fish and 2) an alternative pollock target strength-length relationship that included observations of age-0 pollock changed abundance estimates by as much as 22%. These findings suggest that more research is needed in these areas to obtain more accurate abundance estimates.

CONTENTS

# INTRODUCTION

Walleye pollock (*Gadus chalcogrammus*, hereafter referred to as pollock) are an important ecological and commercial fish species in the Bering Sea. Pollock are regularly surveyed by the Alaska Fisheries Science Center (AFSC) for stock assessment purposes (Ianelli et al. 2017). Since 1979, AFSC scientists from the Midwater Assessment and Conservation Engineering (MACE) program have conducted acoustic-trawl surveys in June-August to estimate the abundance and distribution of the midwater pollock (age-1 and older) along the eastern Bering Sea (EBS) shelf (e.g., Honkalehto and McCarthy 2015). Because of their ecological importance as a forage fish, and their potential as a leading indicator of pollock recruitment, age-0 pollock (e.g., young-of-the-year) have also been surveyed in the EBS using trawl surveys in 2004-2007 (Moss et al. 2009), and acoustic-trawl (AT) methods in 2006-2010 (Parker-Stetter et al. 2013) and in 2011-2012 (De Robertis et al. 2014). Because the underlying assumptions and methods differed, the results from the AT surveys conducted in 2006-2010 and the 2011-2012 were not strictly comparable. This report presents estimates of the abundance and distribution of age-0 pollock in the late summer of 2014 using the method of De Robertis et al. (2014), allowing comparison between the results from the 2011, 2012, and the 2014 AT surveys.

# METHODS

An acoustic-trawl (AT) survey was carried out between 17 August and 30 September 2014 during the Bering Arctic Subarctic Integrated Survey (BASIS) of the eastern Bering Sea, which was organized by the AFSC Ecosystem Monitoring and Assessment (EMA) program. The

survey was conducted aboard the NOAA ship *Oscar Dyson*, a 64-m stern trawler equipped for fisheries and oceanographic research.

Acoustic Equipment, Calibration, and Data Collection

Acoustic backscatter measurements were collected 24 hours per day using a Simrad EK60 echosounder (Simrad 2008, Bodholt and Solli 1992) operating five split-beam transducers at frequencies of 18, 38, 70, 120, and 200 kHz. All transducers were mounted on the bottom of the vessel's retractable centerboard, which extended 7.6 m below the surface during the survey. Acoustic data were collected at a nominal ping rate of 2.0 $s^{-1}$, and a pulse length of 0.512 ms. The results presented in this report are based on 38 kHz data with a post-processing $S_v$ integration threshold of –70 dB re 1 $m^{-1}$ applied to ensure comparability with other AFSC surveys (e.g., Honkalehto and McCarthy 2015).

Standard sphere acoustic system calibrations (Foote et al. 1987) were conducted to measure acoustic system performance on two occasions during the preceding pollock summer survey (Honkalehto and McCarthy 2015). A tungsten carbide sphere (38.1 mm diameter) suspended below the centerboard-mounted transducers was used to calibrate the 38-, 70-, 120-, and 200-kHz systems. The tungsten carbide sphere was then replaced with a 64 mm diameter copper sphere to calibrate the 18-kHz system. A two-stage calibration approach was followed for each frequency. On-axis sensitivity (i.e., transducer gain and $s_A$ correction) was estimated from measurements with the sphere placed in the center of the beam following the procedure described in Foote et al. (1987). Transducer beam characteristics (i.e., beam angles and angle offsets) were estimated by moving the sphere in a horizontal plane through the beam and fitting

these data to a second-order polynomial model of the beam pattern using the ER60's calibration utility (Simrad 2008, Jech et al. 2005). The equivalent beam angle is used to characterize the volume sampled by the beam but it was not estimated using this calibration approach because the absolute position of the sphere was unknown (Demer et al. 2015). Thus, the transducer-specific equivalent beam angle measured by the echosounder manufacturer was corrected for the local sound speed (see Bodholt, 2002) and used in data processing. The calibrations did not reveal substantial differences in echosounder sensitivity, so the results from each calibration were averaged in linear units to produce the values of gain and $s_A$ correction applied in post-processing of acoustic data in the present survey.

Survey Design

The primary survey design for the 2014 BASIS survey consisted of a grid of sampling stations at a separation of 0.5° of latitude and 1° of longitude. Surface trawl samples, oceanographic samples, and zooplankton samples were taken at the predetermined stations during daylight hours. Similar grid stations were sampled in 2006-2010 (Parker-Stetter et al. 2013) and in 2011-2012 (De Robertis et al. 2014). The acoustic data were collected opportunistically as the vessel transited between stations. Midwater trawl hauls were periodically taken to sample high-intensity backscatter observed with the echosounder.

Trawl Sampling

Near-surface backscatter was sampled at predetermined locations using a Cantrawl rope trawl towed at speeds of ~2 m $s^{-1}$ for 30 min (Moss et al. 2009). The Cantrawl is 198 m long, has a

122 m headrope, and is constructed with ropes at the leading edge of the net followed by meshes tapering from 162 to 1.2 cm (stretched mesh measurement) in the codend liner. The trawl was equipped with floats to keep the headrope near the surface. Vertical net openings and depths during fishing were monitored with a Furuno CN24 acoustic-link netsonde attached to the footrope. A trawl vertical opening of 21.6 ± 3.6 m (mean ± standard deviation) during surface trawling was observed with the netsounde on 10 trawl hauls.

Areas of high midwater backscatter were sampled opportunistically either by using the Cantrawl without the floats (Parker-Stetter et al. 2013) or by using a smaller, twice-modified Marinovich midwater trawl (MM2). The MM2 trawl was configured with a 12 m footrope, 12 m headrope, 30 m bridle, and mesh sizes ranging from 6.35 cm at the trawl opening to 1.91 cm at the codend (stretched mesh measurement) with a 0.3 cm liner. Weight chains were used for the midwater trawls, with 250 lbs on each side for the Cantrawl, and 100 lbs on each side for the MM2. Vertical net openings and depths during midwater fishing were monitored with either a Simrad FS70 third-wire netsounde or a Furuno CN24 acoustic-link netsonde attached to the headrope. The vertical opening of the Cantrawl fishing midwater averaged 16.0 ± 3.1 m. The vertical opening of the MM2 net while trawling in midwater averaged 5.25 ± 0.7 m.

Trawl catches were identified to species, enumerated, weighed, and further processed according to a species-specific protocol. All lengths were measured to the nearest 1.0 millimeter (mm) using an electronic measuring board (Towler and Williams 2010). Standard lengths (SL) were measured for smaller forage fish (e.g., age-0 pollock) and fork lengths (FL) were measured for the larger fish (e.g., age-1+ pollock). Pollock less than 13 cm were considered age-0, or young-

of-the-year, whereas pollock 13 cm and larger were considered age-1+ pollock based on length ranges measured during the 2014 BASIS survey. Undamaged, individual jellyfish were weighed to the nearest 2 grams (g), and the bell diameters were measured. All biological measurements and trawl station information were electronically recorded and stored in the Catch Logger for Acoustic Midwater Surveys (CLAMS) relational database, developed by MACE Program staff.

Acoustic Data Processing

Acoustic backscatter measurements were examined and analyzed using Echoview post-processing software (v.6.1.59.27435). While backscatter data were continually collected during the cruise, data retained for analysis of age-0 abundance were collected

a) at 38 kHz, from 12.5 m from surface to 0.5 m off bottom or 1,000 m (max recording depth);
b) during daytime only (between local sunrise and sunset), minimizing diel changes in target strength and species compositions due to vertical migration of demersal species;
c) while underway and not during station sampling or trawling (vessel speeds greater than 7 knots), limiting potential changes in backscatter associated with behavioral responses to trawling vessels (De Robertis and Wilson 2006);
d) from areas with bottom depth > 30 m to avoid near-shore regions that were not sampled by trawls; and
e) from areas with a type of backscatter that had been sampled by trawls and thus reliably ground-truthed.

Of the total water column backscatter that met criteria a-d, about 17% was excluded in step e) because it did not appear similar to or was not near enough to areas where trawl samples were taken. This backscatter included unidentified midwater and near-bottom backscatter, deep scattering layers, plankton, and surface-turbulence (non-biological backscatter). Most of the excluded backscatter was near-bottom and was likely attributed to adult groundfishes, principally adult walleye pollock (Honkalehto and McCarthy 2015, Lauffenburger et al. 2017). Backscatter that passed criteria a) – e) was echo-integrated into 0.5 nautical mile (nmi) by 5 m depth bins, and stored in a relational database for further analysis of age-0 pollock abundance.

Assigning Biological Data to Backscatter

As in De Robertis et al. (2014), estimates of the size and species composition of organisms from trawl samples and their acoustic scattering properties were used to convert the integrated backscatter into age-0 pollock abundance. This process required each acoustic measurement to be assigned to a trawl catch sample to be used for scaling. For the near-surface backscatter (< 30 m), trawl catch information was automatically assigned from the single nearest surface-trawl. For the midwater backscatter, single or multiple midwater-trawl catches were manually assigned. These midwater assignments depended on the aggregation pattern of the backscatter under scrutiny and the proximity and the tow depth of nearby midwater hauls. On two occasions, when no midwater trawl samples were available to assign to midwater backscatter, nearby surface-trawl catches were used instead. After the trawl catches were assigned to backscatter, the species captured were used to scale the backscatter into age-0 pollock abundance. For the primary abundance analysis, equal trawl selectivity among all captured species and sizes was assumed. A series of target-strength (TS in dB re 1 $m^2$, the echo from an individual animal) to

length relationships taken from the literature (Table 1) were used to estimate the acoustic scattering from each species or species group captured in the trawls. Some species caught in the trawl hauls were excluded from analysis because they were unlikely to be present in the backscatter (i.e., salmonids, Emmett et al. 2004, Parker-Stetter et al. 2013), relatively weak scatterers (i.e., plankton, isopods), or uncommon species (i.e., salmon shark, *Lamna ditropis*) compared to target fish species. Some species were left out of our analysis because the specimens were too damaged for length measurements, which often occurred with some jellyfish (e.g., *Aequorea* spp. and *Staurophora mertensi*). Generally, these exclusions were confined to relatively small fractions of the haul's catch by weight (e.g., < 1%), but for a few hauls, the damaged *Aequorea* genus represented 14-16% of the haul's catch by weight.

Estimating Abundance

The general approach to analyzing backscatter for age-0 pollock abundance observed in 2014 was the same as that used by De Robertis et al. (2014), except that computations for the 2014 data analysis were carried out in a different order to accommodate implementation in a database. As previously described in this document, backscatter was assigned trawl catches. The first step in the abundance analysis involved computing the proportion of fish ($p$) of species $s$ and length $l$ from one or more trawls as

$$p_{s,l} = \sum_t \frac{n_{s,l,t}}{\sum_{s,l} n_{s,l,t}} \Big/ c \,, \qquad (1)$$

where $n$ is the number of fish of species $s$ and length $l$ in trawl $t$, and $c$ is the number of trawls used for scaling. The next step was to compute the backscattering cross-section ($\sigma_{bs}$, $m^2$, TS in dB re 1 $m^2$; MacLennan et al. 2002) for each species and length class (length measurement rounded to nearest cm) using the TS relationships given in Table 1. For species for which the TS

relationship was derived using a different length measurement type than the one used for measuring the trawl catch specimens, an appropriate length-length conversion was applied. Based on repeated individual pollock measurements (n = 80) collected during other MACE Program survey efforts, the following SL-length to FL-length relationship was used for age-0 pollock:

$$FL = 1.091 * SL - 0.078. \quad (2)$$

TS was converted into linear units as

$$\sigma_{bs_{s,l}} = 10^{TS_{s,l}/10}. \quad (3)$$

The overall mean $\sigma_{bs,}$ or $\overline{\sigma_{bs}}$ across all species, lengths, and trawls used for scaling was computed as

$$\overline{\sigma_{bs}} = \sum p_{s,l} \cdot \sigma_{bs_{s,l}}. \quad (4)$$

The $\overline{\sigma_{bs}}$ was then used to scale the measured nautical area backscattering coefficient ($s_A$) for each 0.5 nmi × 5 m acoustic data cell within the backscatter analysis regions as

$$N = {s_A}/{4\pi\overline{\sigma_{bs_t}}} \quad (5)$$

(MacLennan et al. 2002). This yielded the total number of all organisms *N* for each cell, which was proportioned back to species-and length-specific density $d$ in each cell for each species and length as

$$d_{s,l} = Np_{s,l}. \quad (6)$$

The areal density for each 0.5 nmi (individuals nmi$^{-2}$) within the analysis region was computed as by summing the densities ($d_{s,l}$) across all 5 m thick acoustic data cell layers (MacLennan et al. 2002).

A survey grid was used to extrapolate the densities of each species and size observed along the trackline to the total surveyed area. The survey area was divided into a 0.5° latitude and 1° longitude grid, where each grid-cell was centered on the predetermined BASIS sampling grid stations. The area of each grid cell was computed in square nautical miles ($nmi^2$). Shallow areas around land masses (< 30 m) were excluded from the grid's total area. Geographic cells containing less than 10 nmi of trackline were excluded from the analysis to avoid error introduced by high levels of extrapolation in sparsely sampled grid cells. The survey-wide abundance-at-length for each species was computed by averaging the areal density along the trackline within each grid cell, multiplying by the area of the grid cell, and then summing across all grid cells. Although survey-wide abundances were estimated for all species, only estimates for walleye pollock (*Gadus chalcogrammus*) are presented in this report. Biomass-at-length estimates for pollock were computed by multiplying the numbers-at-length by the mean weight-at-length. Weight at a given length class (cm) was estimated from a linear regression of the natural logarithms of the length and weight data (De Robertis and Williams 2008). Length-weight regression parameters for age-1+ pollock (Table 2.) were based on individual fish data collected during the AFSC EBS pollock survey (Honkalehto and McCarthy 2015), and the age-0 parameters were taken from Buchheister et al. (2006) and were based on specimens taken at a similar time of year in the Gulf of Alaska.

To derive the relative acoustic contribution for each species caught in a single trawl, the proportion of backscatter (*PB*) from a given species *s* was computed from the number (*n*) of individuals of that species and length *l* captured in a trawl *t* as

$$PB_{s,t} = \sum_l \frac{n_{s,l,t} \cdot \sigma_{bs_{s,l}}}{\sum_{s,l} n_{s,l,t} \cdot \sigma_{bs_{s,l}}}. \quad (7)$$

Multi-year Age-0 Pollock Abundance Comparison

Age-0 pollock abundance estimates were compared between 2011, 2012, and 2014. To make this comparison, adjustments for two small methodological differences were required:

a) Shallowest depth of integration: In the 2014 survey, the acoustic measurements began at 12.5 m, whereas in the 2011-2012 surveys, acoustic measurements were reported starting at 15 m from the surface. For the multi-year comparisons, the 2014 abundance estimate excludes the estimates between 12.5 and 15 m so that abundance estimates starting 15 m from the surface were compared.

b) Survey coverage: The 2014 analysis was recalculated using the 1° latitude by 1° longitude survey grid used in 2011 and 2012. Based on this grid, the 2014 survey covered a larger area ($8 \times 10^4$ nmi$^2$) than the 2011 survey ($6.5 \times 10^4$ nmi$^2$) but smaller than the 2012 survey ($10 \times 10^4$ nmi$^2$). For the multi-year comparison, only grid cells with an age-0 pollock abundance estimate from all three years were used.

Sensitivity Analysis

The abundance of age-0 pollock was recalculated under three scenarios to determine the sensitivity of survey estimates to analytical methodology and assumptions. The first consisted of making a correction to trawl catch samples using recent experimental estimates of length-dependent escape of fish from the trawl (selectivity). Estimates of selectivity were based on field experiments conducted using the Cantrawl and a modified-Marinovich (MM1) midwater trawl during a survey of the Chukchi Sea in 2013 (De Robertis et al. 2016). While the Cantrawl was

the same net used in the 2014 survey, the MM1 was slightly different and possibly more selective with a shorter intermediate section and larger meshes in the aft section than the MM2 used in this survey. Additionally, the De Robertis et al. (2017) study estimated the trawl selectivity for several small fishes in the Chukchi Sea (e.g., Arctic cod, sand lance), which were primarily less than 12 cm, but it did not estimate selectivity of age-0 pollock, and therefore may not be representative of pollock escapement and herding behavior. Rather than applying a selectivity curve from an individual species studied in the Chukchi Sea, a combined-species length selection curve was derived for each gear type. The resulting curves are shown in Figure 1 and represent proportion of fish in each centimeter (cm) length class entering the trawl (all species caught) that were retained in the codend. To determine the influence of selectivity on survey abundance estimates, the number of fish caught *n* at each length class *l* for each species was divided by the proportion retained *p* as

$$\hat{n}_l = {}^{n_l}/_{p_l}, \tag{8}$$

yielding an estimate of the number that was likely to have entered the trawl ($\hat{n}$), and therefore to have been present in the population targeted by the trawl. The rest of this analysis was identical to the original, primary analysis, except that $\hat{n}$ is substituted for $n$ to derive species and size composition.

A second sensitivity analysis was made by using a separate TS - length model for age-0 pollock, in contrast with the standard pollock model used for all ages in the original analysis. For the original analysis, TS was modeled as a log-linear function of length using the expression

$$TS_L = 20 \log_{10} L - 66, \tag{9}$$

where *L* is fish fork length (cm) (Table 1; Traynor 1996). An alternative age-0 model was derived by fitting only the intercept parameter to *in situ* acoustic observations of TS coupled with trawl catches performed on age-0 pollock in the Gulf of Alaska in May 1990 (Brodeur & Wilson, 1996). From several TS collection events reported in that study, two were selected by examining the catch composition and TS distribution (Fig. 2) using *in situ* TS measurement criteria discussed in Traynor (1996). The new intercept value *i* was derived by minimizing the Sum-of-Squared differences (SS) between the observed mean backscattering cross section ($\bar{\sigma}_{bs} = 10^{(\frac{\overline{TS}}{10})}$) as determined by averaging the *in situ* TS detections from Brodeur & Wilson (1996), and the expected mean backscattering cross section ($\tilde{\bar{\sigma}}_{bs}$) as computed using a TS model of the form in Equation 10 with intercept *i*, transformed to linear units as

$$\tilde{\sigma}_{bs\,j} = 10^{\left(20*\log_{10} L_j - i\right)/10} \tag{10}$$

and

$$\tilde{\bar{\sigma}}_{bs} = \frac{\sum_j \left(\tilde{\sigma}_{bs\,j}\right)}{n}, \tag{11}$$

where *L* is the fork length (cm) of the *j*-th fish caught and *n* is the total number of fish caught. The resulting intercept value for the alternative age-0 pollock model was -64.8 dB re 1 $m^2$. The rest of this analysis was identical to the original, primary analysis, except that -64.8 is substituted for the intercept -66 in Equation 10.

The final sensitivity analysis investigated the effect of scaling all backscatter regions using the single nearest haul's trawl catch instead of assigning one or more trawl catches to backscatter regions based on visual inspection of the echogram and analyst experience. This alternative approach analyzed the backscatter from the midwater layer in the same manner as analysis of the

surface layer, as described in the acoustic analysis section. The rest of this analysis was identical to the original, primary analysis.

## RESULTS

### Catch and Size Composition

The 2014 BASIS acoustic trawl survey encompassed $7.56 \times 10^4$ nmi$^2$ represented by 78 0.5° latitude and 1° longitude grid cells and 1,612 nmi of valid acoustic trackline (Fig. 3). During the survey, 79 surface trawls and 35 midwater trawl hauls (19 using the Cantrawl and 16 using the MM2 trawl) were conducted. Age-0 walleye pollock dominated the aggregate trawl catches by number (Table 3), accounting for 87% for the midwater Cantrawl samples, 94% for the MM2 samples, and 87% for the surface Cantrawl samples. By weight, age-1+ pollock accounted for 62% of the total weight for the midwater Cantrawl samples, whereas the jellyfish, *Chrysaora melanaster*, accounted for 88% of the total weight for the MM2 samples and 80% for the surface Cantrawl samples.

Catch composition varied over the survey region. By number, age-0 pollock dominated the majority of inshore catches, where seafloor depths were shallower than 100 m, whereas Atka mackerel and jellyfish were proportionally more abundant in the offshore catches where seafloor depths were greater than 150 m (Fig. 4). *Chrysaora melanaster* and age-1+ gadids (pollock and Pacific cod) comprised most of the total weight of inshore catches, whereas Atka mackerel and jellyfish outranked other species in the offshore hauls (Fig. 5). When the proportion of catch was expressed in terms of acoustic backscatter (relative contribution to backscatter, Equation 7)

(Fig. 6), most of the survey's "catch-backscatter" was due to pollock (age-0 and age-1+). However, in one localized area along the 50 m isobaths, over half of the catch-backscatter was due to adult Pacific cod. Offshore catch-backscatter, near the 200 m isobath, was mostly due to Atka mackerel and other species (e.g., sablefish, prowfish, and juvenile rockfish).

Age-0 pollock ranged in fork length from 2.9 to 12.2 cm with an overall mean length of 6.62 cm. Length samples from the surface and midwater trawls were similar, with a single mode observed at 6.5 cm. Age-0 pollock length measurements from midwater MM2 trawl samples ranged slightly lower (3.2 – 10.3 cm) than midwater Cantrawl samples (3.8 – 12.2 cm). Generally, average lengths at each trawl location were 6 cm or larger across the survey area (Fig. 7). Slightly smaller age-0 pollock, averaging 5 cm, were mostly located in an area southeast of the Pribilof Islands.

Abundance Estimates

Acoustic backscatter observed along the trackline was highest inshore, where bottom depths were < 100 m (Fig. 8). Near-bottom and unidentified backscatter (excluded from abundance estimates) was substantial in the more easterly region of the survey between the 50 m and 70 m isobaths. In general, the highest backscatter that was attributed to species occurred in areas where age-0 pollock or age-1+ pollock dominated the trawl catches (compare Figs. 6 and 8).

The overall abundance estimate for age-0 pollock was $6.85 \times 10^{11}$ fish, comprising a biomass of 2.1 million metric tons (t), with an estimated mean length of 6.61 cm FL (Fig.9). Age-0 pollock accounted for 92.4% of the total abundance among all species analyzed. *Chrysaora melanaster*

represented the second highest abundance at 3.5%, followed by other jellyfish (non-*C. melanaster*) at 1.2%, and age-1+ pollock at 1.2%. The highest age-0 pollock densities were in regions where the mean bottom depth was < 75 m, whereas the highest age-1+ pollock densities were mostly found in areas where bottom depths were > 60 m (Fig. 10).

In 2014, age-0 pollock were the most abundant species in the analyzed portion of the water column, particularly in the upper 30 m, where nearly half (47%) of the estimated abundance was observed (Fig. 11A). Although some larger pollock were also in the upper 30 m (31% by number, 20% by biomass), most of them were deeper (Fig. 11B). For the backscatter analyzed in the survey area, the abundance-weighted mean depth was 37 m for age-0 pollock and 52 m for age-1+ pollock.

Sensitivity Analyses

Relative to the primary analysis results, the sensitivity analyses exhibited negative and positive effects on the age-0 biomass and abundance estimates, and entirely negative effects on age-1+ pollock biomass and abundance estimates (Table 4; Fig. 12A,B). The largest negative effect on age-0 pollock occurred after applying an alternate TS-model for age-0 pollock, which resulted in a 22% decrease in the biomass and abundance. The largest positive effect occurred by adjusting the estimates for trawl selectivity, which resulted in an 11% increase in biomass and a 22% increase in abundance for age-0 pollock, shifting the modal length of age-0 pollock from 7 cm to 6 cm (Fig. 12B). For the larger, age-1 + pollock, trawl selectivity decreased the biomass by 52% and abundance by 45%. This effect is due to the shift in relative proportion of age-0 and larger pollock, which means following the selectivity correction, less of the backscatter can be

attributed to larger pollock thereby reducing their abundance. Finally, using the nearest haul for scaling all of the backscatter yielded a relatively minor (< 10%), negative effect on the biomass and abundance for age-0 and age-1+ pollock (Table 4).

Multi-year Grid-cell Comparison of Age-0 Pollock Abundance

Age-0 pollock abundance from 2011 to 2012, and 2014 was compared using 28 common grid cells among the three survey years (Fig. 13A), representing $5.36 \times 10^4$ $nmi^2$ of surveyed area. In this area, the age-0 pollock abundance estimate was $5.4 \times 10^{11}$ fish for 2014, which was about 3.6 times higher than in 2012, and 8.7 times higher than in 2011. A comparison of the south – north gradient in abundance across survey years (e.g., A-7, B-7, C-7, and D-7) shows that the population observed in 2014 was distributed farther north in shallower waters as compared to 2011-2012 (Fig. 13B).

## DISCUSSION

This report documents the findings from the 2014 acoustic-survey for age-0 pollock in the Bering Sea, which was the third acoustic-trawl survey conducted by the AFSC MACE Program in collaboration with the EMA Program. In comparison to the previous surveys conducted in 2011-2012 (De Robertis et al. 2014), the overall age-0 pollock abundance estimate for 2014 was the highest (3.5 times higher than in 2012, and 9 times higher than 2011). Yet while recruitment of the 2014 year class in the Bering Sea pollock stock has been unremarkable, the 2012 year class appears to be one of the largest observed (Ianelli et al. 2017) indicating that the age-0 abundance estimates reported here were not predictive of year-class strength. Heintz et al. (2013)

found a positive correlation between the average-energy-content (AEC: kJ/fish) of age-0 pollock and age-1 recruits-per-spawner, but this relationship also did not forecast the large 2012 year-class (Heintz et al. 2017).

This report documents the findings from the 2014 acoustic-survey for age-0 pollock in the Bering Sea, which was the third acoustic-trawl survey conducted by the AFSC MACE Program in collaboration with the EMA Program. In comparison to the previous surveys conducted in 2011-2012 (De Robertis et al. 2014), the overall age-0 pollock abundance estimate for 2014 was the highest observed (3.5 times higher than in 2012, and 9 times higher than 2011). Yet recruitment of the 2014 year class in the Bering Sea pollock stock has been unremarkable, while the 2012 year class appears to be one of the largest observed (Ianelli et al. 2017). Although the estimated abundance of age-0 pollock presented in this paper did not forecast age-1 pollock recruitment, Heintz et al. (2013) found a positive correlation between the average-energy-content (AEC: kJ/fish) of age-0 pollock and age-1 recruits-per-spawner. However, due to the relatively low AEC in 2012, the large 2012 year class was not forecast (Heintz et al. 2017).

Annual Changes in Abundance and Species Dominance

In 2014, age-0 pollock were the most abundant species caught in the midwater and surface tows (Table 3). This contrasts with previous surveys in 2011 and 2012 where the dominant catch species were different, particularly in the surface tows. In the 2011 surface trawls, age-0 cod was the most abundant species, and in 2012, capelin was the most abundant species (De Robertis

et al. 2014), yet neither of these species were abundant in 2014 (< 0.1% of the aggregate catch by number in midwater and surface tows). These findings suggest that substantial inter-annual differences in composition of forage fish may be expected.

Uncertainty in Backscatter Classification

About half of the trawl hauls that caught age-0 pollock also caught larger pollock, indicating that different-sized pollock were often present in the same region of the water column during the 2014 survey. These cases presented challenges in interpreting the backscatter, specifically in delineating the different pollock size classes. Where it was possible, fish schools were separated to the different-sized fish based on the backscatter appearance. For example, the larger pollock often formed discrete high backscatter aggregations often termed “cherry-balls” for their appearance on the echograms. In contrast, age-0 pollock had diverse backscatter patterns in 2014, which included instances of “cherry-ball” aggregation types, making it possible that some fish schools were misinterpreted. The presence of the larger pollock distributed throughout the 2014 survey area was expected given the findings of the MACE EBS survey of age-1+ pollock in June-August 2014 (Honkalehto and McCarthy 2015). The effect of classification uncertainty on 2014 age-0 pollock estimates given here is difficult to quantify directly and represents a potential limitation in applying an acoustic survey approach for age-0 pollock in years when the spatial overlap with larger pollock (or other strong acoustic scatterers) is substantial. Although multifrequency methods indicate that discriminating between schools of age-0 pollock and adult pollock is unlikely (De Robertis et al. 2010), broadband acoustic methods might discriminate between individuals or schools of small and large swimbladdered fish. This improved

discriminatory ability would be derived from using wider bandwidth signals to identify resonant or near-resonant scattering from young-of-the-year fish. For example, Bassett et al. (2017) (Fig. 7), which used wideband scattering techniques, observed scattering at and near resonance in a relatively narrow bandwidth around 18 kHz that was consistent with the size and swimbladder geometries reported for young-of-the year pollock (Coyle and Pinchuck 2002 and Dougherty et al. 2007).

Improvements to Surveys of Age-0 Pollock

The report on the 2011 and 2012 surveys (De Robertis et al. 2014) set out a series of recommendations for future surveys on age-0 pollock in the Bering Sea. This survey incorporated several of these recommendations, which included using a smaller trawl to sample backscatter. The MM2 trawl provided a sampling option in poor weather conditions when the much larger CanTrawl could not be operated. While the retention properties of the MM2 with respect to age-0 pollock were not directly evaluated in this survey, the modifications to the original Marinovich trawl were specifically designed with the intent to improve retention of similarly-sized young-of-the-year fishes in the Chukchi Sea surveys (De Robertis, per. comm.). Another recommendation was to increase the number of targeted midwater trawl samples. During the 2014 survey, the number of targeted midwater trawl samples increased 1.6 times from the 2012 survey, improving backscatter identification. Several of the sensitivity analyses from the previous report were repeated, which provided insight into the influence of certain analysis approaches and assumptions, and provided contrast with previous surveys (Table 4).

Target Strength of Age-0 Pollock

Applying a standard pollock TS-length function (Traynor 1996) to age-0 pollock assumes that the backscatter properties derived by analyzing *in situ* observations of primarily adult pollock can be extrapolated to lengths corresponding to age-0 pollock. This assumption may not be valid, as substantial external morphological differences between these size groups are apparent. These differences may result in a different relationship between fish length and swim bladder shape (the primary sound scattering organ) that departs from the log-linear relationship between length and TS observed in age-1+ pollock (Bassett, pers. comm., 3 April 2018). Fewer *in situ* observations of age-0 pollock have been made in which individual fish targets can be distinguished and other acoustically visible organisms are not present. The data points used for this analysis were collected in 1990, and out of many TS collections during that cruise, only two were found to be suitable for TS model fitting. Using an age-0 specific TS relationship results in a substantial reduction in age-0 abundance (22 %), as the higher intercept value for the TS length function (-64.8 dB re 1 $m^2$) implied greater individual reflectivity per individual, and therefore fewer individual age-0 pollock per unit backscatter. Continued use of the standard pollock TS relationship maintains comparability with previous BASIS efforts but is probably not as accurate as using a TS relationship that has been demonstrated to be appropriate for age-0 pollock. Implementing an alternative TS model would require more TS observations on age-0 pollock to improve confidence in the parameter estimates.

Trawl Selectivity

Trawl selectivity has been shown to have strong effects on some pollock surveys (Williams 2013) and likely impacted the abundance estimates of age-0 pollock during this survey. When

trawl selectivity models from De Robertis et al. (2017) were applied, the estimated abundance of age-0 pollock increased by 22% and abundance-at-length was shifted toward smaller fish (Fig. 12 B) relative to the original, primary analysis.

The results validated the expectation that the MM2 trawl would better retain fish in the size range of age-0 pollock than the Cantrawl (used in 2011 and 2012), reducing the overall survey-level effects from the combined trawl samples. However, since trawl selectivity models from De Robertis et al. (2017) were based on a different species, they may not correctly represent pollock escapement and herding behavior. Hence, this trawl selectivity correction was not included in the original, primary abundance assessment.

Assignment of Trawl Catch to Classified Backscatter

Considerable analysis effort was spent deciding which trawl catches to use for scaling specific backscatter regions. A sensitivity analysis was used to contrast analyst assignments with direct spatial-based assignment of trawl-catch to backscatter, removing the manual review of trawl-catch, length-composition, and backscatter pattern. The results show that the effects on overall age-0 pollock abundance were relatively minor (4% decrease), but a larger effect was observed on larger pollock biomass (9% decrease). These results were similar to the sensitivity analyses carried out for the 2011 and 2012 data by De Robertis et al. (2014), where the nearest haul approach was evaluated. As the objectives of this survey are to derive a best estimate of age-0 pollock abundance, direct assignment of the nearest trawl catch to backscatter may be an acceptable approach, when analyst time is limited.

In conclusion, the results of this survey form a short, but informative abundance time series of an important component of the Bering Sea ecosystem, and demonstrate the process of making improvements in survey methodology that will hopefully continue as future monitoring efforts are undertaken.

## ACKNOWLEDGMENTS

The authors are indebted to Adam Spear and Matt Wilson, staff with the AFSC Midwater Assessment and Conservation Engineering and Ecosystem Monitoring and Assessment groups, and the many participants of the 2014 BASIS surveys for their varied contributions to many aspects of this work. The work would not have been possible without the efforts of the officers and crew of the NOAA ship *Oscar Dyson*.

# REFERENCES

Bassett, C., A.D. Robertis, and C.D. Wilson, 2017. Broadband echosounder measurements of the frequency response of fishes and euphausiids in the Gulf of Alaska. ICES J. Mar. Sci., 75:1131-1142.

Bodholt, H., 2002. The effect of water temperature and salinity on echo sounder measurements. ICES Symposium on Acoustics in Fisheries, Montpellier 10–14 June 2002.

Bodholt, H., and H. Solli. 1992. Split beam techniques used in Simrad EK500 to measure target strength, p.16-31. *In* World Fisheries Congress, May 1992, Athens, Greece.

Brodeur, R. D., and M. T. Wilson. 1996. Mesoscale acoustic patterns of juvenile walleye pollock (*Theragra chalcogramma*) in the Western Gulf of Alaska. Can. J. Fish. Aquat. Sci. 53:1951-1963.

Buchheister, A., M.T. Wilson, R.J. Foy, and D. A. Beauchamp. 2006. Seasonal and geographic variation in condition of juvenile walleye pollock in the western Gulf of Alaska. Trans. Am. Fish. Soc. 135:897-907.

Coyle, K.O., and A.I. Pinchuk. 2002. The abundance and distribution of euphausiids and zero-age pollock on the inner shelf of the southeast Bering Sea near the Inner Front in 1997-1999. Deep-sea Res. II. 49:6009-6030.

Demer, D.A., L. Berger, M. Bernasconi, E. Bethke, K. Boswell, D. Chu, R. Domokos, A. Dunford, S. Fässler, S. Gauthier, L.T. Hufnagle, J.M. Jech, N. Bouffant, A. Lebourges-Dhaussy, X. Lurton, G.J. Macaulay, Y. Perrot, T. Ryan, S. Parker-Stetter, S. Stienessen, T. Weber, and N. Williamson. 2015. Calibration of acoustic instruments. ICES Coop. Res. Rep. 326, 133 p.

De Robertis, A., D.R. McKelvey, and P.H. Ressler. 2010. Development and application of an empirical multifrequency method for backscatter classification. Can. J. Fish. Aquat. Sci. 67:1459-1474.

De Robertis, A., D. McKelvey, K. Taylor, and T. Honkalehto. 2014. Development of acoustic-trawl survey methods to estimate the abundance of age-0 walleye pollock in the eastern Bering Sea shelf during the Bering Arctic Subarctic Integrated Survey. U.S. Dep. Commer., NOAA Tech. Memo. NMFS-AFSC-272, 46 p.

De Robertis, A., and K. Taylor. 2014. *In situ* target strength measurements of the scyphomedusa *Chrysaora melanaster*. Fish. Res. 153:18-23.

De Robertis, A., K. Taylor, K. Williams, and C.D. Wilson. 2017. Species and size selectivity of two midwater trawls used in an acoustic survey of the Alaska Arctic. Deep-sea Res. II. 135:40-50.

De Robertis, A., K. Taylor, C.D. Wilson, E. V. Farley. 2016. Abundance and distribution of Arctic cod (*Boreogadus saida*) and other pelagic fishes over the continental shelf of the Alaskan northern Bering and Chukchi Seas. Deep-sea Research II. 135:51-65.

De Robertis, A., and K. Williams. 2008. Weight-length relationships in fisheries studies: the Standard allometric model should be applied with caution. Trans. Am. Fish. Soc. 137:707-719.

De Robertis, A., and C. D. Wilson. 2006. Walleye pollock respond to trawling vessels. ICES J. Mar. Sci. 63:514-522.

Dougherty, A.B., K.M. Bailey, and K.L. Mier. 2007. Interannual differences in growth and hatch date distributions of age-0 year walleye pollock *Theragra chalcogramma* (Pallas) sampled from the Shumagin Islands region of the Gulf of Alaska, 1985-2001. J. Fish Biol. 71:763-780.

Emmett, R. L., R. D. Brodeur, and P. M. Orton. 2004. The vertical distribution of juvenile salmon (*Oncorhynchus* spp.) and associated fishes in the Columbia River plume. Fish. Oceanogr. 13:392-402.

Foote, K. G. 1987. Fish target strengths for use in echo integrator surveys. J. Acoust. Soc. Am. 82:981-987.

Foote, K. G., H. P. Knudsen, G. Vestnes, D. N. MacLennan, and E. J. Simmonds. 1987. Calibration of acoustic instruments for fish density estimation. ICES Coop. Res. Rep. 144, 81 p.

Gauthier, S., and J. K. Horne. 2004. Acoustic characteristics of forage fish species in the Gulf of Alaska and Bering Sea based on Kirchhoff-approximation models. Can. J. Fish. Aquat. Sci. 61:1839-1850.

Guttormsen, M. A., and C. D. Wilson. 2009. *In situ* measurements of capelin (*Mallotus villosus*) target strength in the North Pacific Ocean. ICES J. Mar. Sci. 66:258-263.

Heintz, R.A., E.C. Siddon, and E.V. Farley. 2017. Fall Energetic Condition of Age-0 Walleye Pollock Predicts Survival and Recruitment Success, p 151-153. *In*: Siddon and Zador (Eds.), Ecosystem Considerations 2017, Status of the Eastern Bering Sea Marine Ecosystem. Pacific Fishery Management Council, 605 West 4th Ave., Suite 306, Anchorage, AK 99501. Available from: https://www.afsc.noaa.gov/REFM/Docs/2017/ecosysEBS.pdf

Heintz, R.A., E.C. Siddon, E.V. Farley, and J.M. Napp. 2013. Correlation between recruitment and fall condition of age-0 pollock (*Theragra chalcogramma*) from the eastern Bering Sea under varying climate conditions. Deep-sea Res. II, 94:150-156.

Honkalehto, T., and A. McCarthy. 2015. Results of the acoustic-trawl survey of walleye pollock (*Gadus chalcogrammus*) on the U.S. and Russian Bering Sea shelf in June - August 2014 (DY1407). AFSC Processed Rep. 2015-07, 62 p. Alaska Fish. Sci. Center., NOAA, Natl. Mar. Fish. Serv, 7600 Sand Point Way, NE, Seattle WA 98115.

Ianelli, J., S. Kotwicki, T. Honkalehto, K. Holsman, and B. Fissel. 2017. Assessment of the walleye pollock stock in the eastern Bering Sea, p 55-184. *In* Stock assessment and fishery evaluation report for the groundfish resources of the Bering Sea/Aleutian Islands regions. Pacific Fishery Management Council, 605 West 4th Ave., Suite 306, Anchorage, AK 99501. Available at https://www.afsc.noaa.gov/refm/ Docs/2017/EBSpollock.pdf.

Jech, J.M., K.G. Foote, D. Chu, and L.C. Hufnagle. 2005. Comparing two 38-kHz scientific echosounders. ICES J. Mar. Sci 62:1168-1179.

Kang, D. Y., T. Mukai, K. Iida, D. J. Hwang, and J. G. Myoung. 2005. The influence of tilt angle on the acoustic target strength of the Japanese common squid (*Todarodes pacificus*). ICES J. Mar. Sci. 62:779-789.

Lauffenburger, N., A. De Robertis, and S. Kotwicki. 2017. Combining bottom trawls and acoustics in a diverse semipelagic environment: What is the contribution of walleye pollock (*Gadus chalcogrammus*) to near-bottom acoustic backscatter in the eastern Bering Sea? Can. J. Fish. Aquat. Sci. 74:256–264.

MacLennan, D. N., P. G. Fernandes, and J. Dalen. 2002. A consistent approach to definitions and symbols in fisheries acoustics. ICES J. Mar. Sci. 59:365-369.

Moss, J. H., E. V. Farley, A. M. Feldmann, and J. N. Ianelli. 2009. Spatial distribution, energetic status, and food habits of eastern Bering Sea age-0 walleye pollock. Trans. Am. Fish. Soc. 138:497-505.

Ona, E. 2003. An expanded target-strength relationship for herring. ICES J. Mar. Sci. 60:493-499.

Parker-Stetter, S., J. K. Horne, E. Farley, D. H. Barbee, A. G. Andrews, L. B. Eisner, and J. M. Nomura. 2013. Summer distributions of forage fish in the eastern Bering Sea. Deep-sea Res. II 94:211-230.

Peltonen, H., T. Malinen, and A. Tuomaala. 2006. Hydroacoustic *in situ* target strength of smelt (*Osmerus eperlanus* (L.)). Fish. Res. 80:190-195.

Rose, G. A., and D. R. Porter. 1996. Target-strength studies on Atlantic cod (*Gadus morhua*) in Newfoundland waters. ICES J. Mar. Sci. 53:259-265.

Simrad, 2008. Simrad ER60 scientific echo sounder manual Version Rev. C. Simrad Subsea A/S, Strandpromenaden 50, Box 111, N-3191 Horten, Norway.

Swartzman, G., R. Brodeur, J. Napp, G. Hunt, D. Demer, and R. Hewitt. 1999. Spatial proximity of age-0 walleye pollock (*Theragra chalcogramma*) to zooplankton near the Pribilof Islands, Bering Sea, Alaska. ICES J. Mar. Sci. 56:545-560.

Towler, R., and K. Williams. 2010. An inexpensive millimeter-accuracy electronic length measuring board. Fish. Res. 106:107-111.

Traynor, J. J. 1996. Target strength measurements of walleye pollock (*Theragra chalcogramma*) and Pacific whiting (*Merluccius productus*). ICES J. Mar. Sci. 53:253-258.

Williams, K. 2013. Evaluation of midwater trawl selectivity and its influence on acoustic-based fish population surveys. University of Washington. Seattle WA. 166 p.

Yasuma, H., R. Nakagawa, T. Yamakawa, K. Miyashita, and I. Aoki. 2009. Density and sound-speed contrasts, and target strength of Japanese sandeel *Ammodytes personatus.* Fish. Sci. 75:545-552.

Table 1.-- Target strength to size relationships from the literature used to allocate 38 kHz acoustic backscatter to species in this study. The symbols in the equations are as follows: $a$ is the bell radius (m), $L$ is length (cm), $Z$ is depth (m).

| **Species or group** | **TS** (dB re 1 $m^2$) | **TS derived for which species** | **Reference** |
|---|---|---|---|
| Gadids | $TS = 20 \log_{10}L - 66$ | *Gadus chalcogrammus* *Gadus morhua* | Traynor 1996, Rose and Porter 1996 |
| Capelin | $TS = 20 \log_{10}L - 70.3$ | *Mallotus villosus* | Guttormsen and Wilson 2009 |
| Jellyfish | $TS = 10 \log_{10}(\pi a^2) - 46.8$ | *Chrysaora melanaster* | De Robertis and Taylor 2014 |
| Sand lance | $TS = 56.5 \log_{10}L - 125.1$ | *Ammodytes personatus* | Yasuma et al. 2009 |
| Smelts | $TS = 20 \log_{10}L - 65.9$ | *Osmerus eperlanus* | Peltonen et al. 2006 |
| Squid | $TS = 20 \log_{10}L - 75.4$ | *Todarodes pacificus* | Kang et al. 2005 |
| Herring | $TS = 20 \log_{10}L - 67.4 - 2.3 \log_{10}(1 + z/10)$* | *Clupea harengus* | Ona et al. 2003 |
| Atka mackerel | $TS = 18.5 \log_{10}L - 81$ | *Pleurogrammus monopterygius* | Gauthier and Horne 2004 |
| Other fishes | $TS = 20 \log_{10}L - 67.4$ | physoclists | Foote 1987 |

* Herring TS formula requires an input for depth; for this analysis, the depth was fixed at 10 m.

Table 2. -- Least-squares linear regression parameters of $\log_e$ transformed organism length (L; cm) and $\log_e$ transformed whole-body wet weight (W; g) used to estimate biomass for pollock observed during the 2014 BASIS survey.

| Organism | Reference or data source | $\log_e (W) = b \log_e (L) - a$ | | |
|---|---|---|---|---|
| | | *L* | *a* | *b* |
| Pollock (age-0) | Buchheister et. al. 2006 | standard length | 11.485 | 2.958 |
| Pollock (age-1+) | Honkalehto and McCarthy 2015 | fork length | 11.594 | 2.935 |

Table 3. -- Catch by species from 79 near surface Cantrawl hauls (A), 19 midwater Cantrawl hauls (B), and 16 midwater Marinovich hauls (C) during the 2014 survey. Less abundant species were pooled into the 'other' category. Immature and juvenile salmon were grouped.

**A. Cantrawl - surface**

| | | | | Weight | |
|---|---|---|---|---|---|
| Common name | Scientific name | Number | (%) | (kg) | (%) |
| walleye pollock (age-0) | *Gadus chalcogrammus* | 668,001 | 87.0 | 1,504.5 | 3.8 |
| walleye pollock (age-1+) | *Gadus chalcogrammus* | 39,638 | 5.2 | 2,347.6 | 5.9 |
| sea nettle | *Chrysaora melanaster* | 28,298 | 3.7 | 31,612.1 | 79.9 |
| Atka mackerel | *Pleurogrammus monopterygius* | 10,211 | 1.3 | 828.1 | 2.1 |
| sablefish | *Anoplopoma fimbria* | 6,762 | 0.9 | 294.1 | 0.7 |
| sockeye salmon | *Oncorhynchus nerka* | 4,167 | 0.5 | 766.9 | 1.9 |
| hydromedusa | *Aequorea* sp. | 2,132 | 0.3 | 430.1 | 1.1 |
| Pacific herring | *Clupea pallasi* | 1,561 | 0.2 | 210.8 | 0.5 |
| Pacific cod (0-age) | *Gadus macrocephalus* | 1,261 | 0.2 | 4.9 | < 0.1 |
| rockfish (0-age) | *Sebastes* sp. | 1,143 | 0.1 | 1.0 | < 0.1 |
| chum salmon | *Oncorhynchus keta* | 573 | 0.1 | 535.9 | 1.4 |
| jellyfish | *Cyanea* sp. | 572 | 0.1 | 176.4 | 0.4 |
| capelin (age-0) | *Mallotus villosus* | 518 | 0.1 | 0.3 | < 0.1 |
| lion's mane | *Cyanea capillata* | 500 | 0.1 | 95.4 | 0.2 |
| greenling | Hexagrammidae (family) | 469 | 0.1 | 2.1 | < 0.1 |
| capelin | *Mallotus villosus* | 436 | 0.1 | 1.8 | < 0.1 |
| Pacific sandfish | *Trichodon trichodon* | 299 | < 0.1 | 25.7 | 0.1 |
| whitecross jellyfish | *Staurophora mertensii* | 249 | < 0.1 | 101.3 | 0.3 |
| prowfish | *Zaprora silenus* | 206 | < 0.1 | 5.5 | < 0.1 |
| sand lance | Ammodytidae (family) | 146 | < 0.1 | 1.4 | < 0.1 |
| yellowfin sole | *Limanda aspera* | 118 | < 0.1 | 58.8 | 0.1 |
| squid | Teuthida (order) | 106 | < 0.1 | 0.2 | < 0.1 |
| Chinook salmon | *Oncorhynchus tshawytscha* | 102 | < 0.1 | 167.7 | 0.4 |
| other | | 354 | < 0.1 | 369.5 | 0.9 |
| Totals | | 767,822 | | 39,542.0 | |

Table 3. -- Continued.

**B. Cantrawl - midwater**

| Common name | Scientific name | Number | (%) | Weight (kg) | Weight (%) |
|---|---|---|---|---|---|
| walleye pollock (age-0) | *Gadus chalcogrammus* | 468,331 | 87.3 | 1,217.2 | 10.6 |
| walleye pollock (age-1+) | *Gadus chalcogrammus* | 64,755 | 12.1 | 7,072.3 | 61.6 |
| sea nettle | *Chrysaora melanaster* | 2,444 | 0.5 | 2,776.6 | 24.2 |
| Pacific cod | *Gadus macrocephalus* | 226 | < 0.1 | 300.4 | 2.6 |
| jellyfish (unidentified) | | 221 | < 0.1 | 1.7 | < 0.1 |
| capelin | *Mallotus villosus* | 182 | < 0.1 | 0.7 | < 0.1 |
| Pacific cod (age-0) | *Gadus macrocephalus* | 124 | < 0.1 | 0.7 | < 0.1 |
| other | | 366 | 0.1 | 115.6 | 1.0 |
| Totals | | 536,649 | | 11,485.2 | |

**C. Marinovich - midwater**

| Common name | Scientific name | Number | (%) | Weight (kg) | Weight (%) |
|---|---|---|---|---|---|
| walleye pollock (age-0) | *Gadus chalcogrammus* | 124,829 | 93.9 | 228.0 | 5.6 |
| sea nettle | *Chrysaora melanaster* | 5,554 | 4.2 | 3,563.7 | 87.7 |
| walleye pollock (age-1+) | *Gadus chalcogrammus* | 882 | 0.7 | 188.1 | 4.6 |
| Pacific cod (age-0) | *Gadus macrocephalus* | 590 | 0.4 | 1.8 | 0.0 |
| hydromedusa | *Aequorea* sp. | 544 | 0.4 | 2.8 | 0.1 |
| lion's mane | *Cyanea capillata* | 170 | 0.1 | 35.1 | 0.9 |
| capelin (age-0) | *Mallotus villosus* | 154 | 0.1 | 0.1 | < 0.1 |
| other | | 285 | 0.2 | 44.6 | 1.1 |
| Totals | | 133,008 | | 4,064.1 | |

Table 4. -- Effect of changing post-processing parameters on estimated pollock abundance and biomass observed during the 2014 BASIS survey.

| Alternative analysis considered | % Change relative to the primary analysis | | | |
|---|---|---|---|---|
| | Age-0 | | Age-1+ | |
| | Abundance | Biomass | Abundance | Biomass |
| Apply alternative target strength model to age-0 pollock | - 22 | -22 | - 8 | - 6 |
| Add trawl selectivity | + 22 | +11 | - 45 | -52 |
| Assign nearest midwater haul to midwater zone | - 4 | - 3 | - 2 | - 9 |

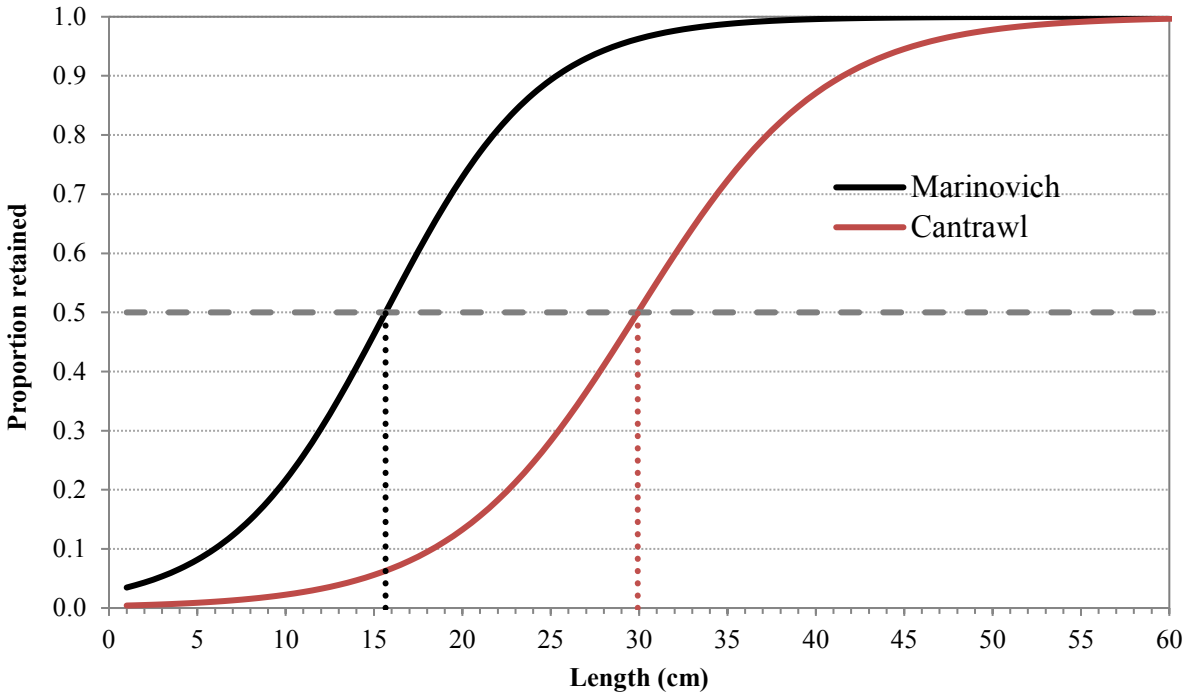


Figure 1.-- Size-dependent logistic selectivity function applied to the Marinovich and Cantrawl nets as part of the alternate scenarios considered. The length-at-50% retention (L50) was set to 15.65 cm and 29.92 cm for the Marinovich and Cantrawl, respectively. The selection range (SR; length (cm) between 25% and 75% retention) was set to 9.67 and 11.61 cm for the Marinovich and Cantrawl, respectively. These data were based on De Robertis et al. (2015).

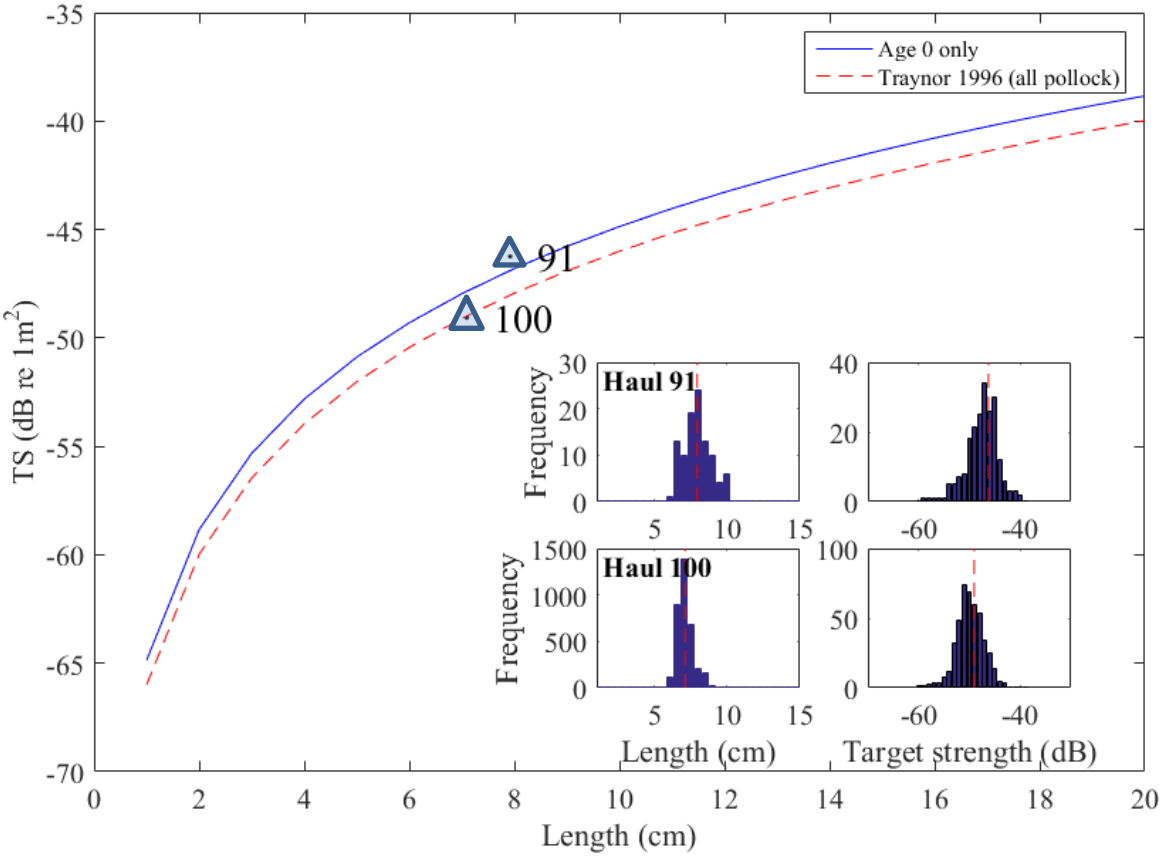


Figure 2.--Target-strength (dB) as a function of fork length (cm) for walleye pollock < 20 cm in length illustrated using the Traynor (1996) model (red-dash line) and the age-0 only model (blue-line). The age-0 only model was derived using *in situ* target-strength (TS) measurements for age-0 pollock observed during hauls 91 and 100 (Brodeur and Wilson 1996). The length and TS averages for the *in situ* TS measurements are illustrated on the histogram plots as vertical red-dash lines, and presented on the TS-length model plot as triangles.

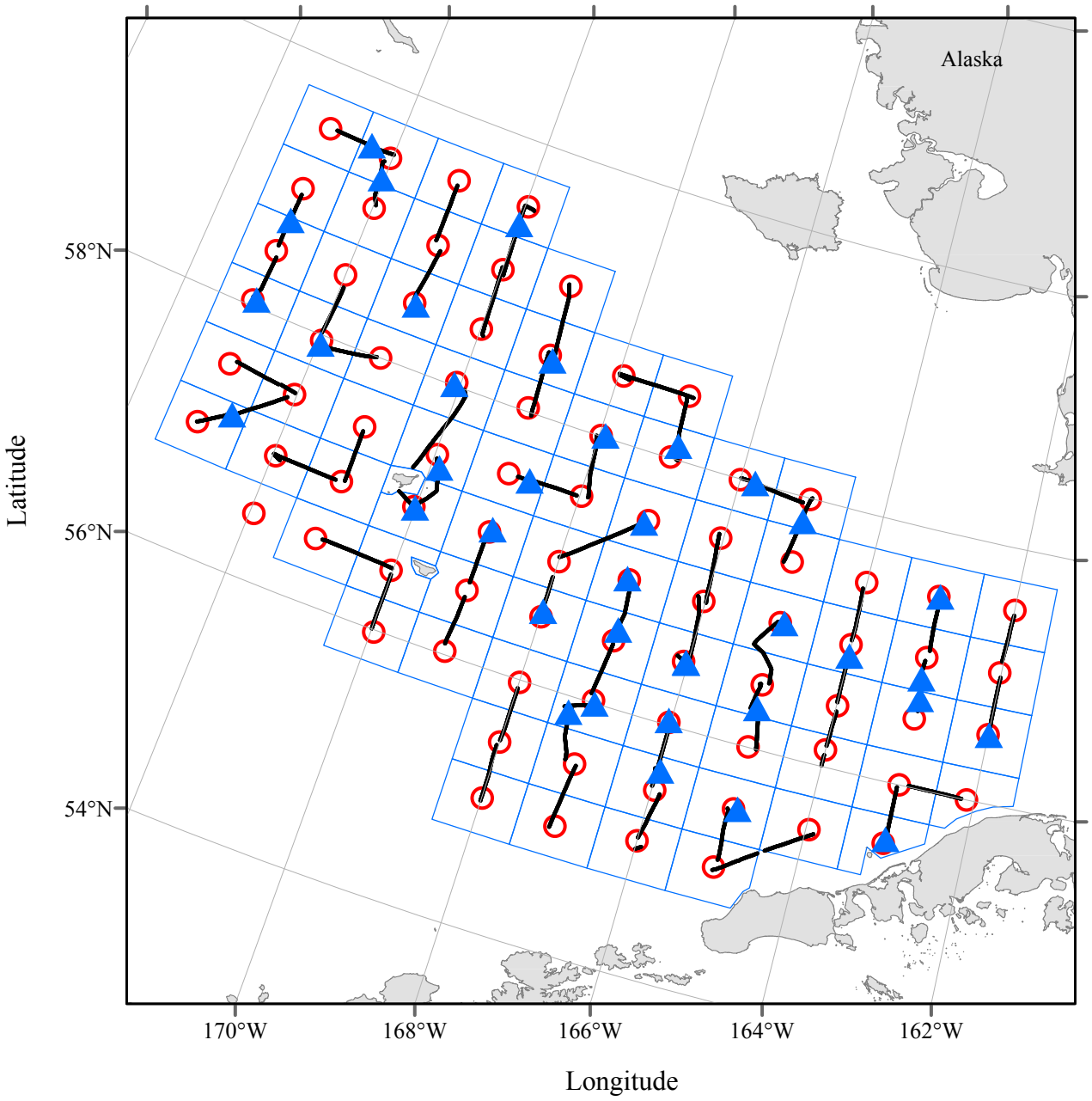


Figure 3.--The grid used in data analysis and a map of survey effort during the 2014 BASIS survey. The acoustic data in each 1 degree longitude by 30 minute latitude grid cell (pictured as blue grid) was extrapolated over the grid cell area if > 10 nmi of acoustic trackline were available in the cell. Acoustic tracklines (black lines), locations of surface trawls (red cirles), and targeted midwater trawls (blue triangles) are indicated.

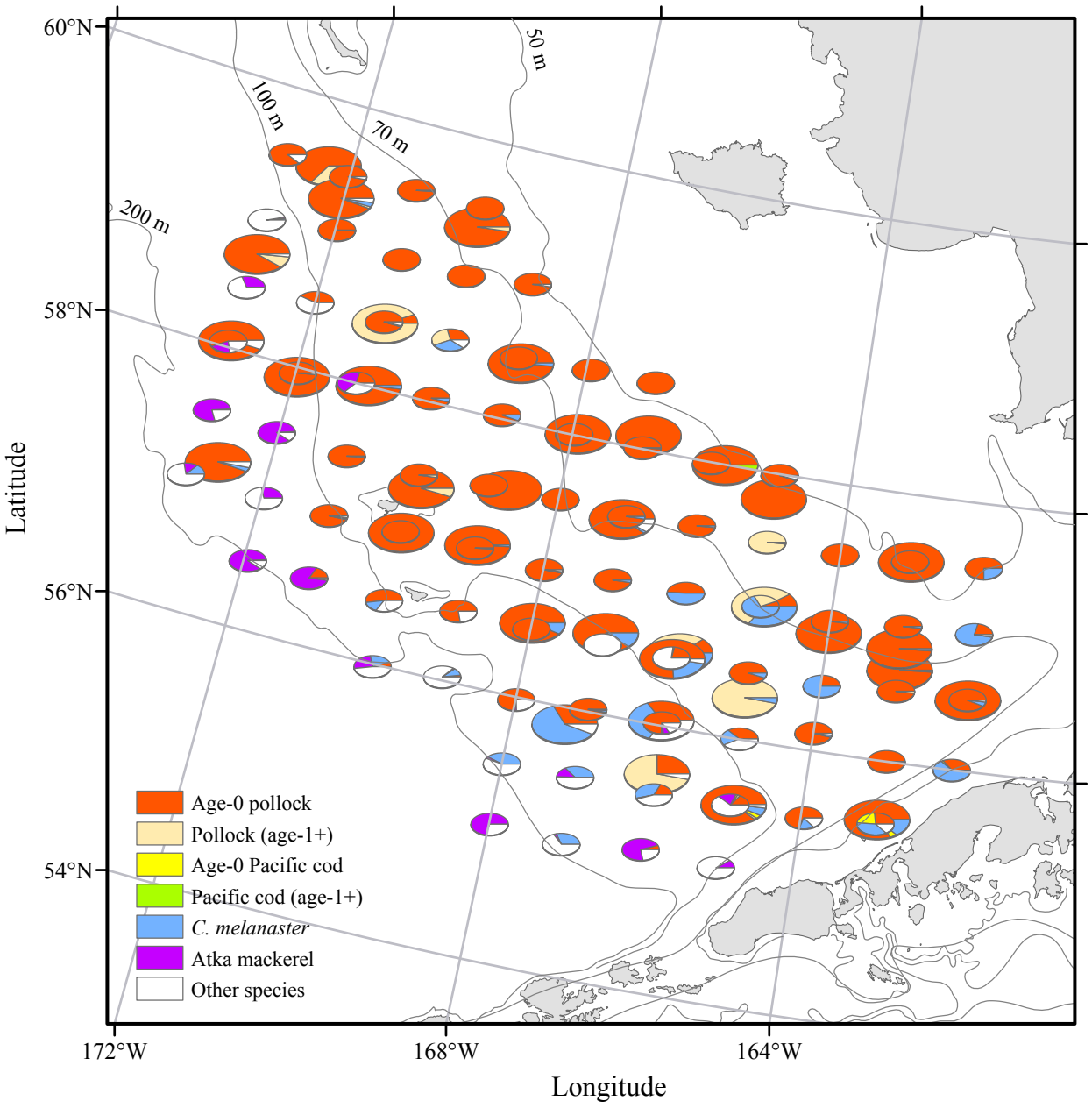


Figure 4.-- Catch composition expressed as proportion of catch by individuals caught during the BASIS survey in 2014. The larger pie graphs represent midwater trawl hauls and the smaller ones represent surface trawls.

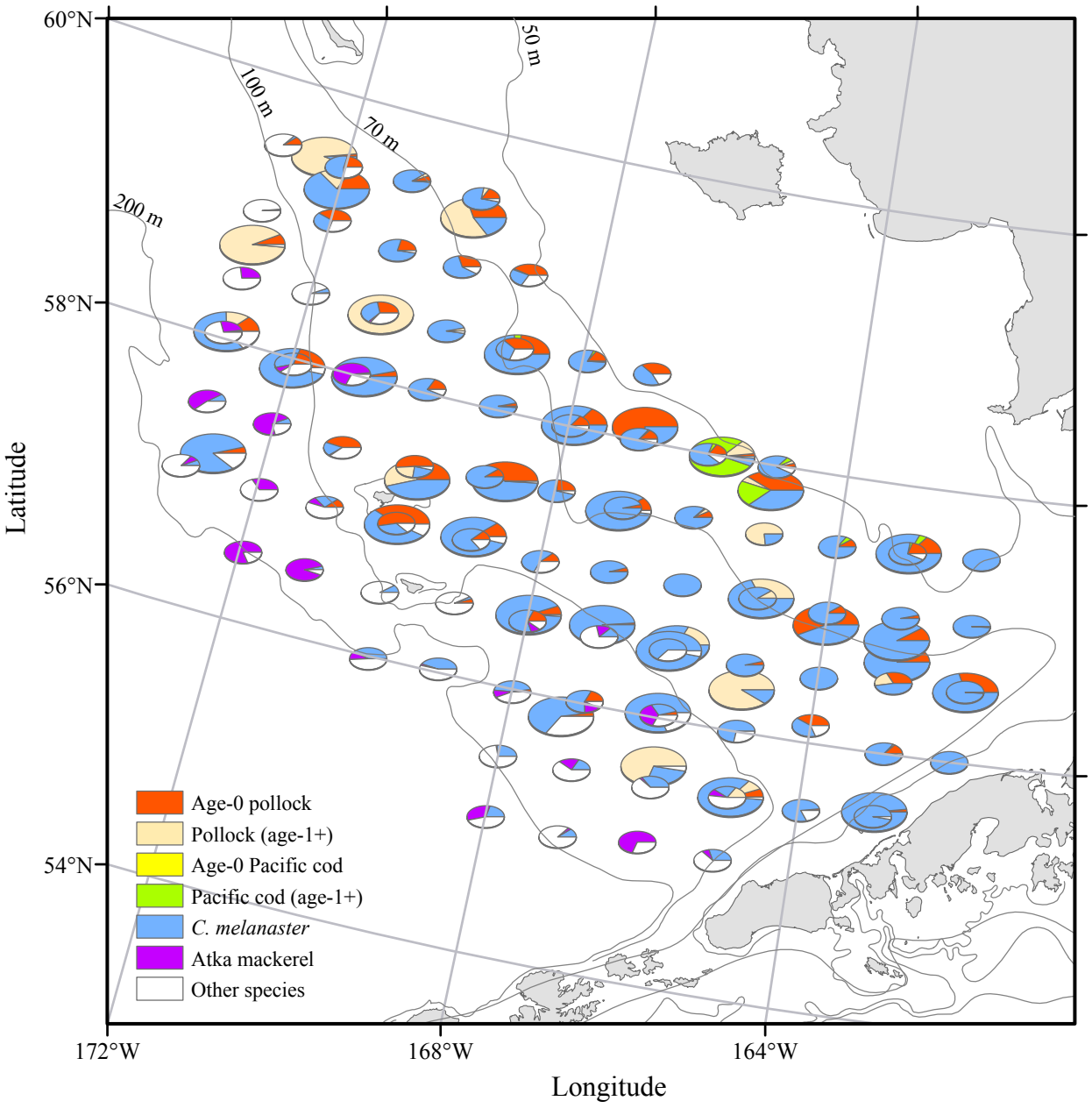


Figure 5.-- Catch composition expressed as proportion of catch by weight caught during the BASIS survey in 2014. The larger pie graphs represent midwater trawl hauls and the smaller ones represent surface trawls.

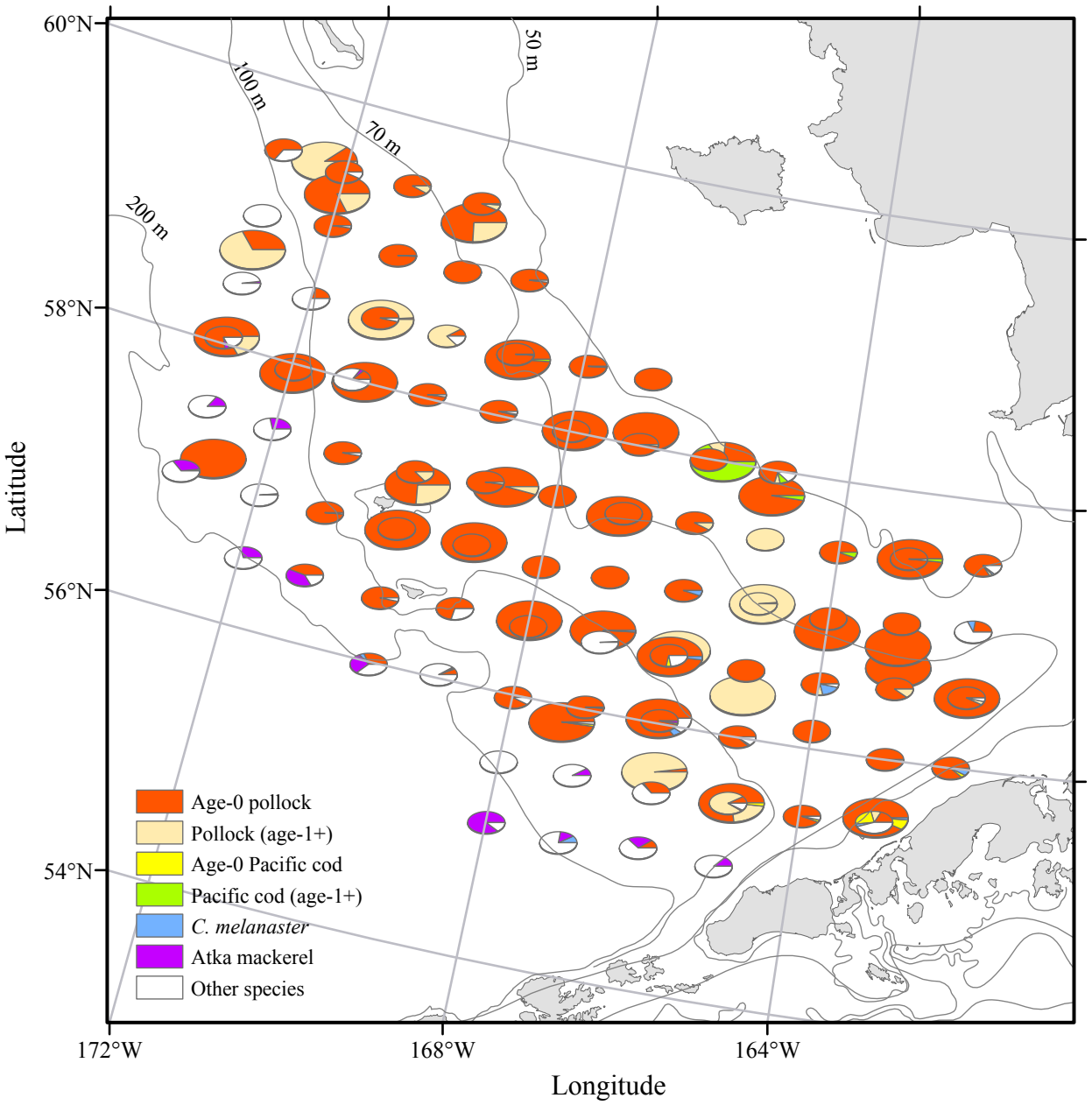


Figure 6.-- Estimated proportion of backscatter attributable to key species derived by combining estimates of species composition from trawl catches and estimates of target strength listed in Table 1 for the BASIS survey in 2014. The larger pie graphs represent estimates for midwater trawl hauls and the smaller ones represent surface trawls.

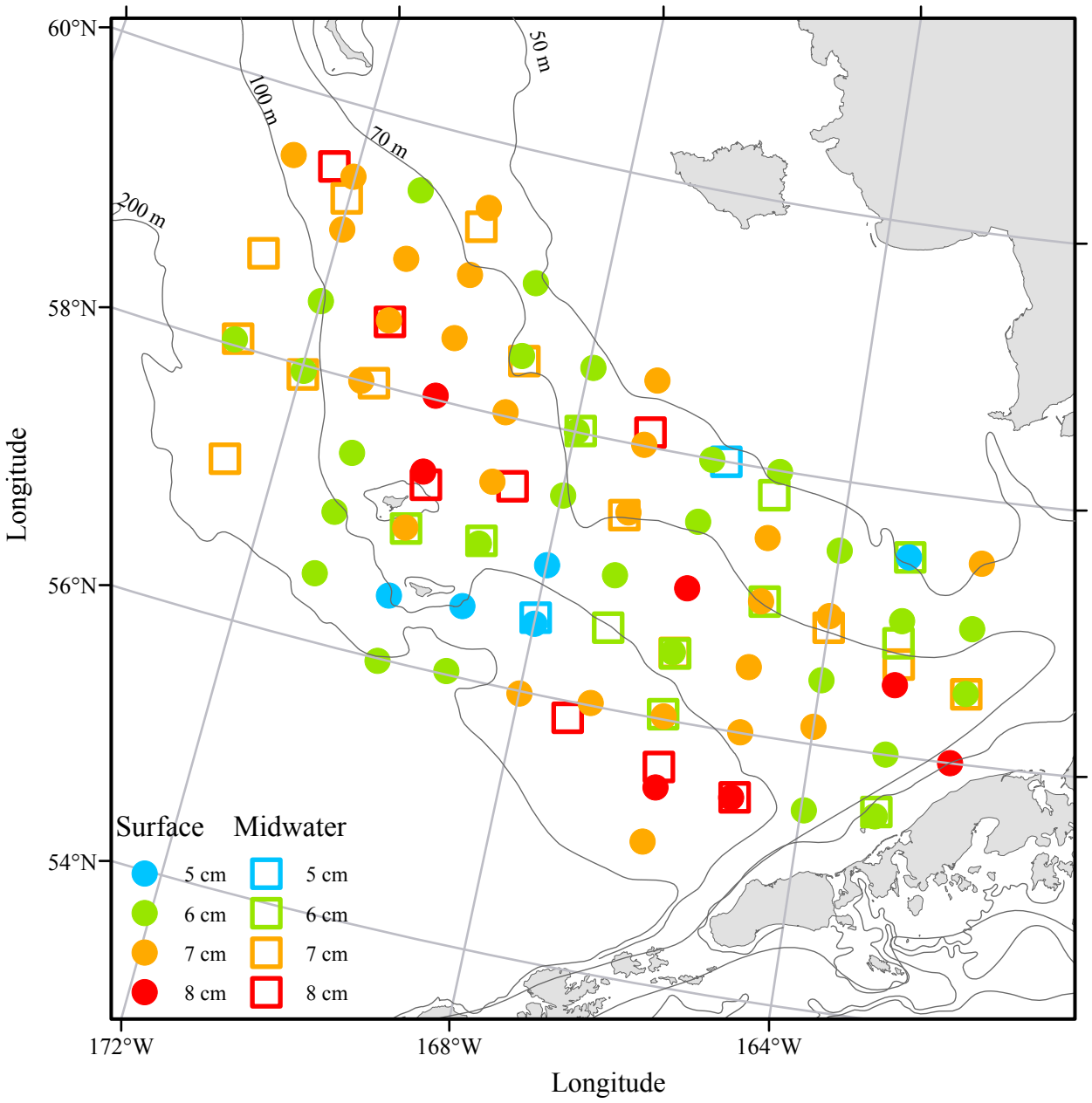


Figure 7.-- Age-0 pollock average fork length (cm) at locations sampled by midwater (squares) and surface trawls (circle).

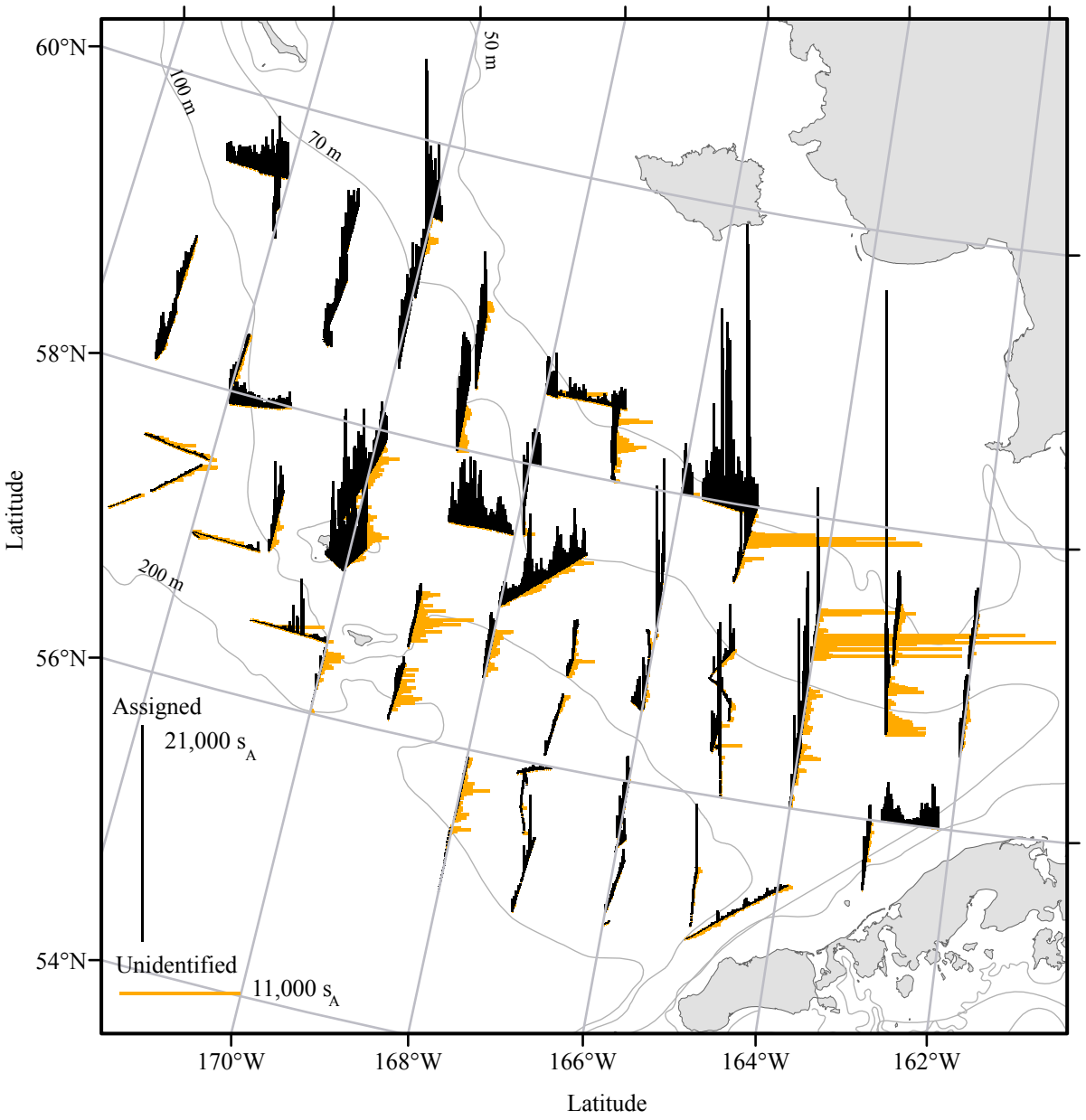


Figure 8.-- Integrated 38 kHz backscatter ($s_A$, $m^2/nmi^2$) measured between 12.5 m from the surface to 0.5 m above the bottom along the vessel track during the 2014 BASIS survey. Black bars illustrate the distribution of backscatter that was assigned to species and the orange bars illustrate the unidentifieded backscatter (near-bottom, unidentified fish, plankton).

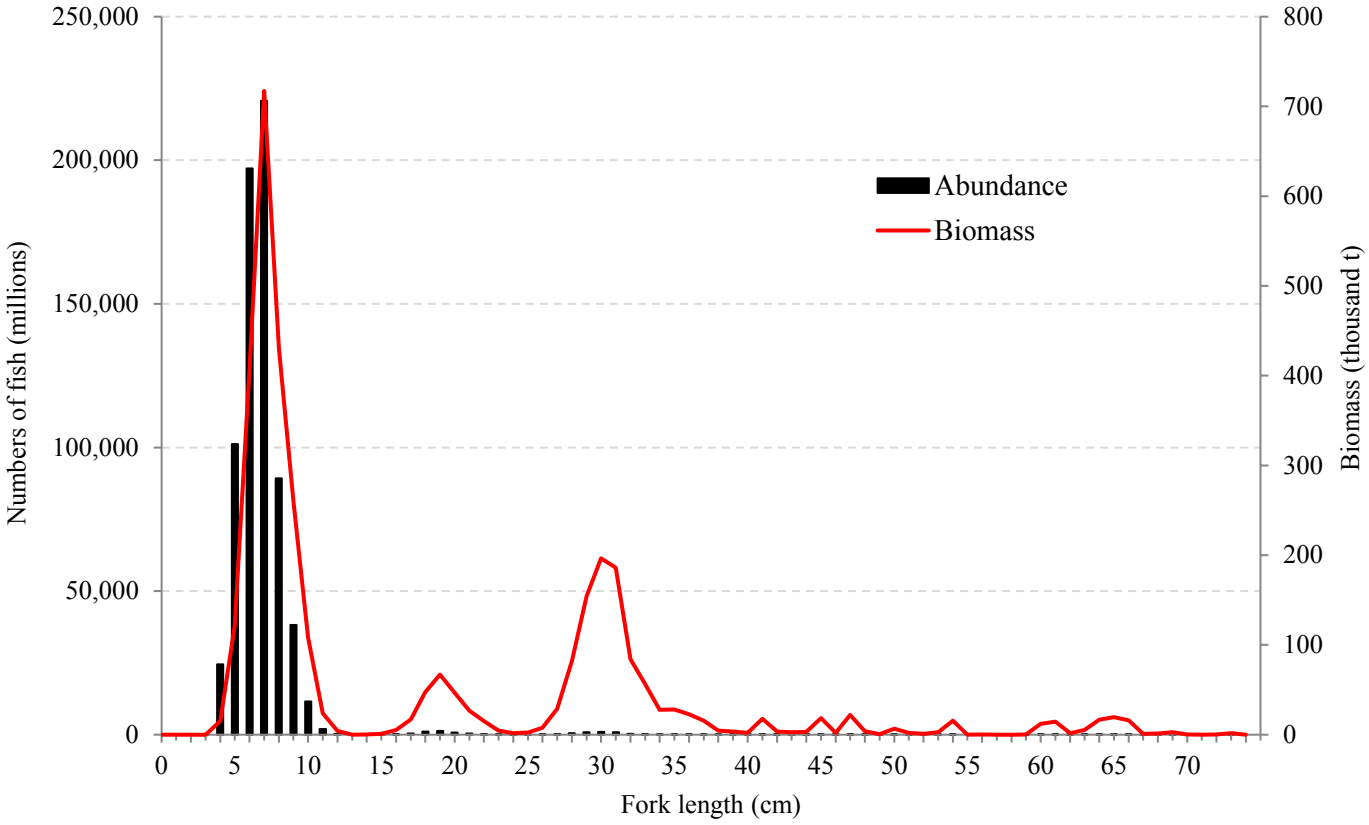


Figure 9.--Estimated pollock population numbers (millions) and biomass (thousand t) at length (cm) observed during the 2014 BASIS survey.

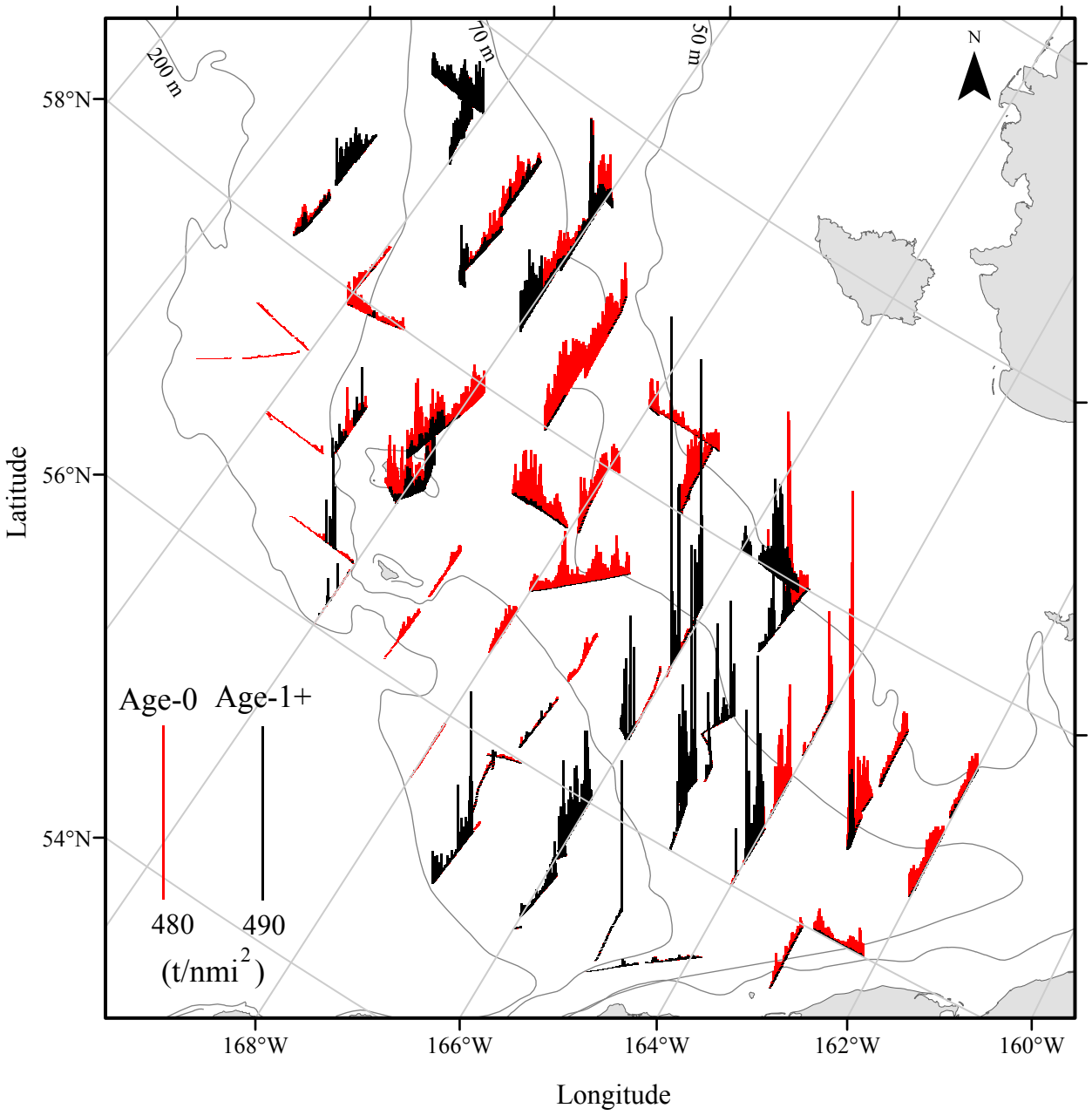


Figure 10.-- Age-0 pollock (red) and age-1+ pollock (black) density estimates (biomass, t/nmi$^2$) along tracklines during the 2014 BASIS survey.

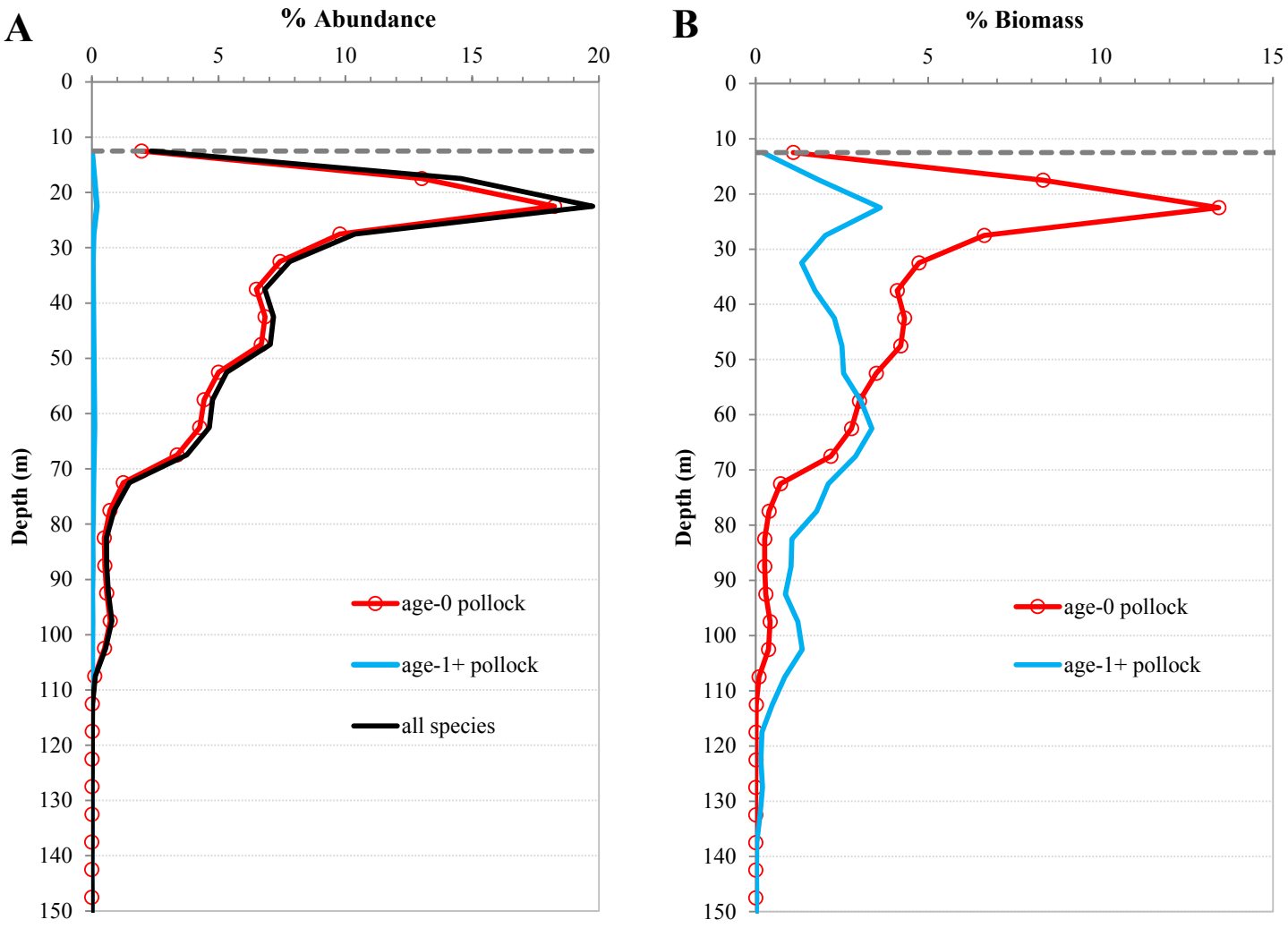


Figure 11.--Relative abundance by depth estimated for pollock, and all species combined ( A) and relative biomass by depth estimated for pollock (B) for the portion of the water column analyzed. Estimates shallower than 12.5 m (above dotted grey line) are not available.

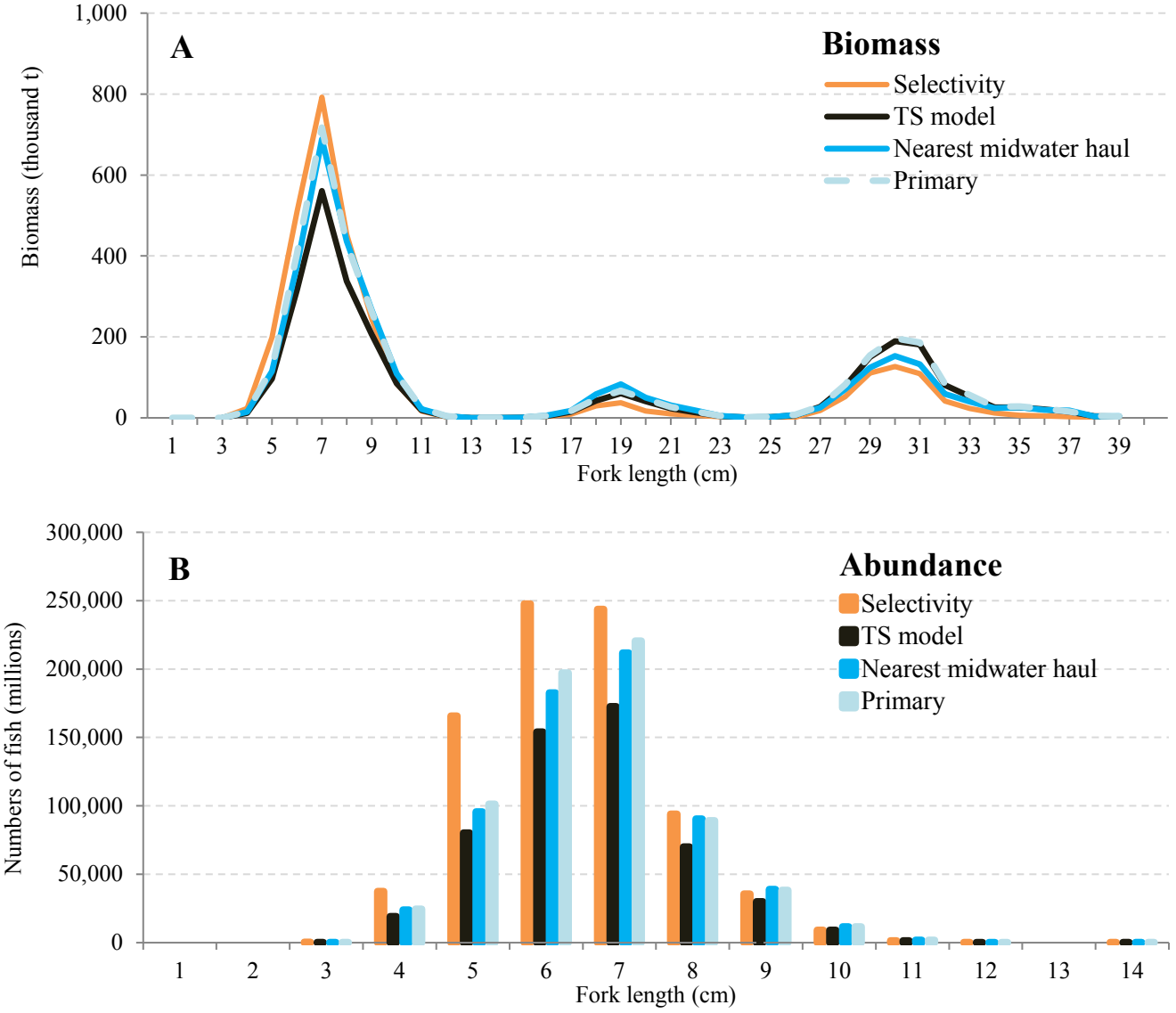


Figure 12.-- Midwater pollock population biomass (thousand t) (A) and numbers (millions) (B) at length from the primary analysis compared to the sensitity analysis (selectivity, age-0 target strength (TS) model, nearest midwater hauls). Pollock biomass comparisons are illustrated for fish < 40 cm (A), and pollock abundance comparisons are illustrated for fish < 15 cm (B)).

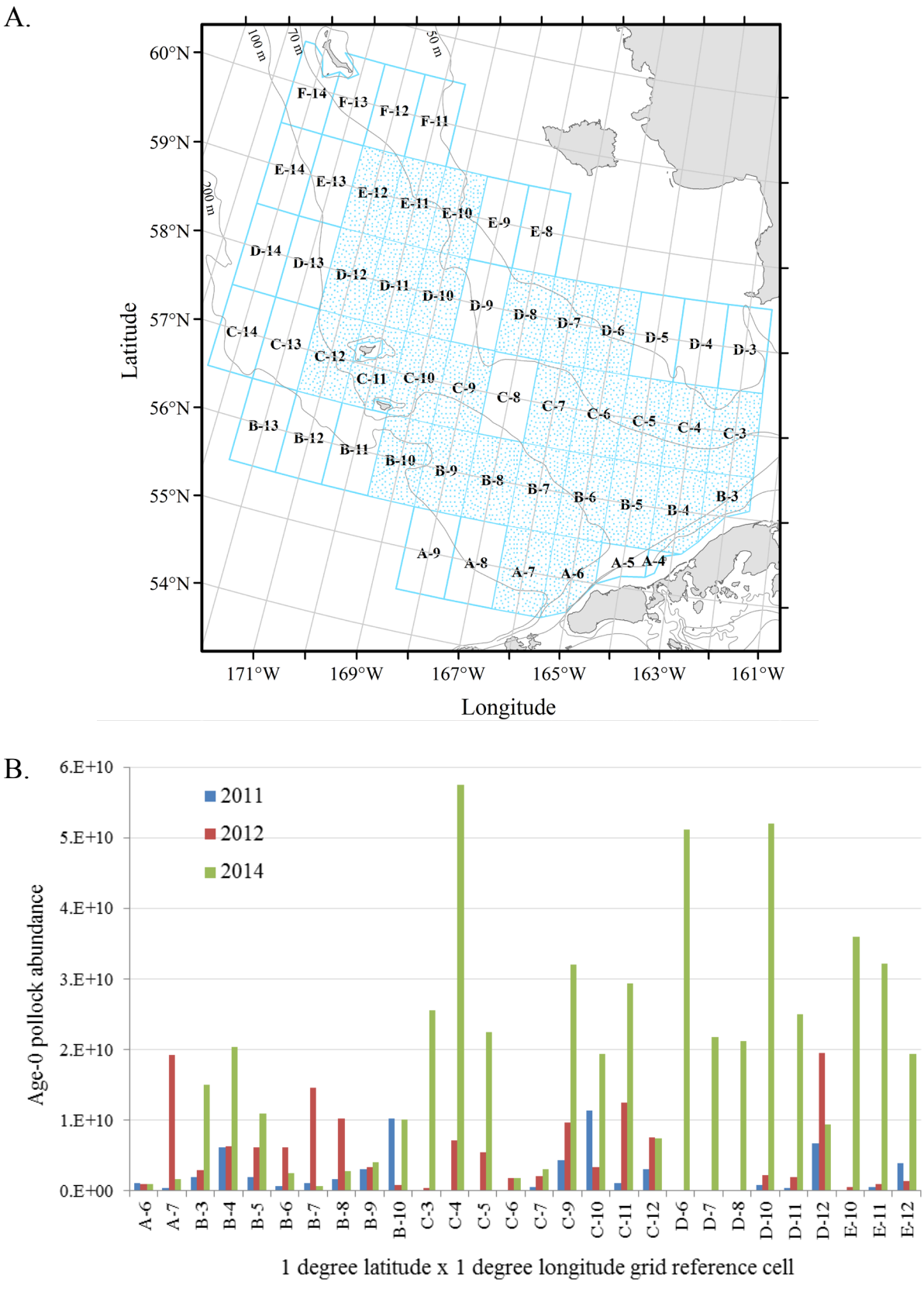


Figure 13.--Reference grid-cells for comparing the estimated abundance of age-0 pollock during the 2011, 2012, and 2014 BASIS surveys (A), where the shaded cells are common among all three surveys. Histogram of estimated age-0 pollock abundance for the shaded cells (B).

# RECENT TECHNICAL MEMORANDUMS

Copies of this and other NOAA Technical Memorandums are available from the National Technical Information Service, 5285 Port Royal Road, Springfield, VA 22167 (web site: *www.ntis.gov)*. Paper and electronic (.pdf) copies vary in price.

AFSC-

381 MCKELVEY, D., and K. WILLIAMS. 2018. Abundance and distribution of age-0 walleye pollock in the eastern Bering Sea shelf during the Bering Arctic Subarctic Integrated Survey (BASIS) in 2014, 48 p. NTIS number pending.

380 SEUNG, C. K., and S. MILLER. 2018. Regional economic analysis for North Pacific fisheries, 86 p. NTIS number pending.

379 GANZ, P., S. BARBEAUX, J. CAHALAN, J. GASPER, S. LOWE, R. WEBSTER, and C. FAUNCE. 2018. Deployment performance review of the 2017 North Pacific Observer Program, 68 p. NTIS number pending.

378 M. M. MUTO, V. T. HELKER, R. P. ANGLISS, B. A. ALLEN, P. L. BOVENG, J. M. BREIWICK, M. F. CAMERON, P. J. CLAPHAM, S. P. DAHLE, M. E. DAHLHEIM, B. S. FADELY, M. C. FERGUSON, L. W. FRITZ, R. C. HOBBS, Y. V. IVASHCHENKO, A. S. KENNEDY, J. M. LONDON, S. A. MIZROCH, R. R. REAM, E. L. RICHMOND, K. E. W. SHELDEN, R. G. TOWELL, P. R. WADE, J. M. WAITE, and A. N. ZERBINI. 2018. Alaska marine mammal stock assessments, 2017, 272 p. NTIS number pending.

377 RICHWINE, K. A., K. R. SMITH, and R. A. MCCONNAUGHEY. 2018. Surficial sediments of the eastern Bering Sea continental shelf: EBSSED-2 database documentation, 48 p. NTIS No. PB2018-101013.

376 DORN, M. W., C. J. CUNNINGHAM, M. T. DALTON, B. S. FADELY, B. L. GERKE, A. B. HOLLOWED, K. K. HOLSMAN, J. H. MOSS, O. A. ORMSETH, W. A. PALSSON, P. A. RESSLER, L. A. ROGERS, M. A. SIGLER, P. J. STABENO, and M. SZYMKOWIAK. 2018. A climate science regional action plan for the Gulf of Alaska, 58 p. NTIS No. PB2018-100998.

375 TESTA, J. W. (editor). 2018. Fur seal investigations, 2015-2016, 107 p. NTIS No. PB2018-100966.

374 VON SZALAY, P. G., and N. W. RARING. 2018. Data Report: 2017 Gulf of Alaska bottom trawl survey, 266 p. NTIS No. PB2018-100892

373 ROONEY, S., C. N. ROOPER, E. LAMAN, K. TURNER, D. COOPER, and M. ZIMMERMANN. 2018. Model-based essential fish habitat definitions for Gulf of Alaska groundfish species, 370 p. NTIS No. PB2018-100826.

372 LANG, C. A., J. I. RICHAR, and R. J. FOY. 2018. The 2017 eastern Bering Sea continental shelf and northern Bering Sea bottom trawl surveys: Results for commercial crab species, 233 p. NTIS No. PB2018-100825.

371 RODGVELLER, C. J., K. B. ECHAVE, P-J. F. HULSON, and K. M. COUTRÉ. 2018. Age-at-maturity and fecundity of female sablefish sampled in December of 2011 and 2015 in the Gulf of Alaska, 31 p. NTIS No. PB2018-100824.